Storage Capacity in Step Pool Stormwater Conveyance Systems

Carriage Hills Tributary, Annapolis, MD

by John Whelan
Advisors: Dr. Karen Prestegaard, Rosemary Fanelli
GEOL 394

TABLE OF CONTENTS

Abstract

The increase in impervious ground cover due to suburban and urban development causes an increase in storm runoff and adjustments in stream channel morphology. Stream restoration projects are installed with the goal of reducing the negative effects excess runoff produces. A relatively new method of stream restoration is a Step Pool Storm Conveyance System. SPSC systems are a sequences of permeable steps and pools installed in an incised channel that is intended to reduce energy of surface storm water flow. This reduction in energy should lead to a reduction in channel erosion and an increase water travel times. As storm water is ponded in the various pools, it may infiltrate into the subsurface and flow through the system as subsurface flow. This method of restoration is commonly installed in or near the heads of first-order streams. Previous studies on similar step pool stormwater management systems indicate that they mitigate the runoff response for low magnitude events (Palmer et al. 2013). This study focuses on the infiltration rates and groundwater responses in a Maryland SPSC system to determine whether the water storage capacity of the system is limited by the infiltration rate or the available storage. Surface infiltration measurements tests indicated that although each pool has a sandy base, the infiltration rates are lower than expected for sandy sediments. Groundwater wells fitted with pressure transducers were used to evaluate the head response to storm events and evapotranspirative demand.

I) Introduction

First-order streams are often erosive because they tend to have the steepest gradients in the watershed. Head-cut erosion by overland flow tends to further steepen stream headwaters as steep hillslopes are converted into stream channels. This headward migration often results in bed incision (Yu 2010). These erosive processes are often significant in urban areas where stormwater runoff has been directed into the heads of small channels that may themselves be consequences of agricultural-era erosion (Wolman, 1967). Effective storm runoff comes from impervious surfaces (roads, parking lots) in urban and suburban areas that are routed directly to streams via storm sewers. . The total percentage of these surfaces in the watershed increases with urban development, which contributes to overland flow runoff and thus erosion (Leopold, 1968, Hammer, 1972). In order to combat channel degradation, stream restoration projects have been implemented in many regions, including the Chesapeake Bay Watershed (Palmer and Allen, 2006).

Figure 1: Channel incision present in adjacent un-restored stream

With an increase in impervious area of 10-20%, the amount of runoff in a system can double (Leopold, 1968). In addition, the time between peak precipitation and peak runoff (lag time) is shortened in urbanized environments. This leads to an increase in flood events with shorter duration and higher discharge. This increase in surface flow often results in channel widening or incision to accommodate for higher discharges (Hammer, 1972; Paul & Meyer, 2001).

Stream channel heads form in the landscape at sites where surface or subsurface flow can generate erosion (Montgomery and Dietrich, 1988). Channel initiation can result from either overland flow that detaches particles from the soil or from subsurface runoff that causes seepage failures. Channel initiation by subsurface runoff involves the cohesiveness of soil and pore water pressure, components of soil strength. As subsurface runoff is increased, pore pressure in the soil is also increased, which reduces the effective normal stress and strength of the soil. In cohesionless (e.g. sandy) soils, this decrease in soil strength can lead to soil failure and channel head initiation (Dietrich & Montgomery, 1988). Channel heads play a crucial role in the morphology of a stream. Stream morphology is constantly adapting to environmental changes. One way that streams adapt to changes is through headward erosion. This process effectively lengthens the stream in the opposite direction of flow. This often compensates for changes in flow to keep the system stable (Hancock et al. 2010). Urban

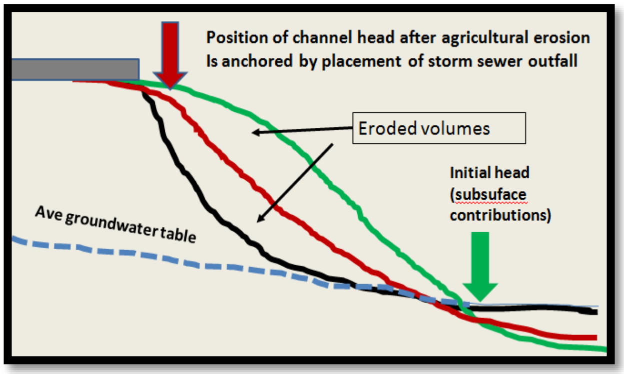

Figure 2: Schematic of erosion due to anchored channel head

storm sewer systems often make the location of channel heads (e.g. drainage pipes outlets from storm drains) permanent, which prevents headward migration or channel filling from occurring. Figure 2 shows how streams might behave after a fixed channel head is installed. Channel erosion is increased when the head is anchored in a fixed location and runoff to the channel is increased by the storm drain outlet. This leads to channel incision, which was present at Carriage Hills prior to restoration with the SPSC system.

Due to the rapid increase in restoration practices, new restoration designs are being implemented in watersheds before they have been monitored or tested extensively (Palmer et al. 2013). For example, Ann Arundel County decided to install a Step Pool Stormwater Conveyance (SPSC) system at Carriage Hills. These SPSC systems are a relatively new technology and they have been designed to store and treat stormwater runoff and prevent further erosion in first-order streams. SPSC systems are composed of a series of engineered pools and steps that are installed in a headwater stream where headward erosion and channel incision has occurred. Step pool morphology is common in high gradient, boulder-bed streams and is effective at dissipating energy at the boulder steps (Wilcox et al. 2006). This stream morphology is common in headwater streams, but not on the Maryland Coastal Plain where boulder-sized sediments are largely absent. The intent of this restoration method is to reduce the kinetic energy of surface stormwater flow by reducing energy gradients (except at the boulder steps) and thus flow velocity. The reduction in flow velocity leads to less erosive forces acting on the stream bed and prevents channel degradation (Chin 2005). Step-pool storm-water systems require both boulders for the steps and sand and gravel fill material for the pool. The sediment size should be fine-grained enough to store storm-water in the pore spaces, but coarse enough to allow the water to drain sufficiently between storm events. Wood chips and other organic matter are incorporated into the fill material to foster low oxygen levels and provide a suboxic environment for denitrification.

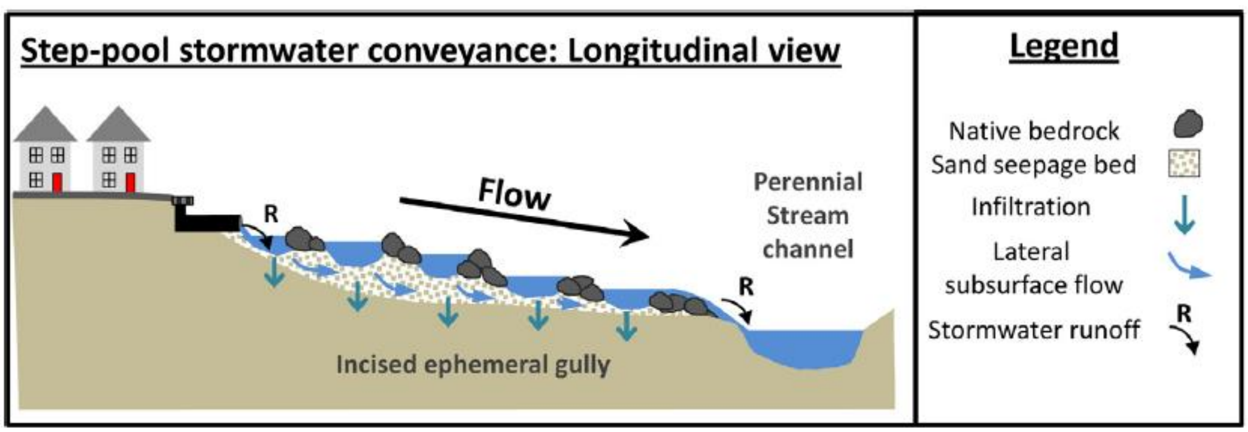

Figure 3: Schematic of flow for SPSC systems (Palmer et al. 2013)

Hydrological response of a watershed is significantly influenced by the water balance, which can be evaluated on storm to annual time-steps. The water balance is a quantification of water inputs, outputs, and storage in the system. For the SPSC system, the inputs are storm water runoff conveyed by the storm drain plus precipitation over the structure. The outputs from the system are stream flow during storm events, groundwater flow, and evapotranspiration. Between storm events outflow is equal to the groundwater flow plus evapotranspiration.

Evapotranspiration demand is the greatest in the summer months and can be minimal during winter months.

The storage in the system is also dependent on the inflow, outflow of surface and groundwater and amount of evapotranspiration. Pool surface storage will undergo a negative change due to evapotranspiration and drainage, and a positive change due to inflow into the system. For changes in subsurface storage, the same applies however there is no evapotranspiration present below the surface.

a) Previous Studies

Carriage Hills tributary is currently being monitored as part of a study of runoff, water quality, and stream ecology in restored and non-restored sites. Precipitation and stream discharge data in addition to nitrogen concentration and conductivity data have been collected at this site. The preliminary data suggest that SPSC systems do alter hydrological processes. Figure 4 shows that the restored stream did experience less runoff responses for storm events less than one inch in magnitude. This suggests that the SPSC system has a capacity to store the runoff that results from 1 inch or less of precipitation on the impervious surfaces in the watershed. Storm events that produced more than one inch (2.54 cm) of precipitation, however, generated similar runoff responses in both the restored and un-restored streams (Palmer et al., 2013). These data suggest that the storage capacity (both surface and subsurface) of the pools is either filled or ineffective when runoff volumes from storm events larger than 2.54 cm occur.

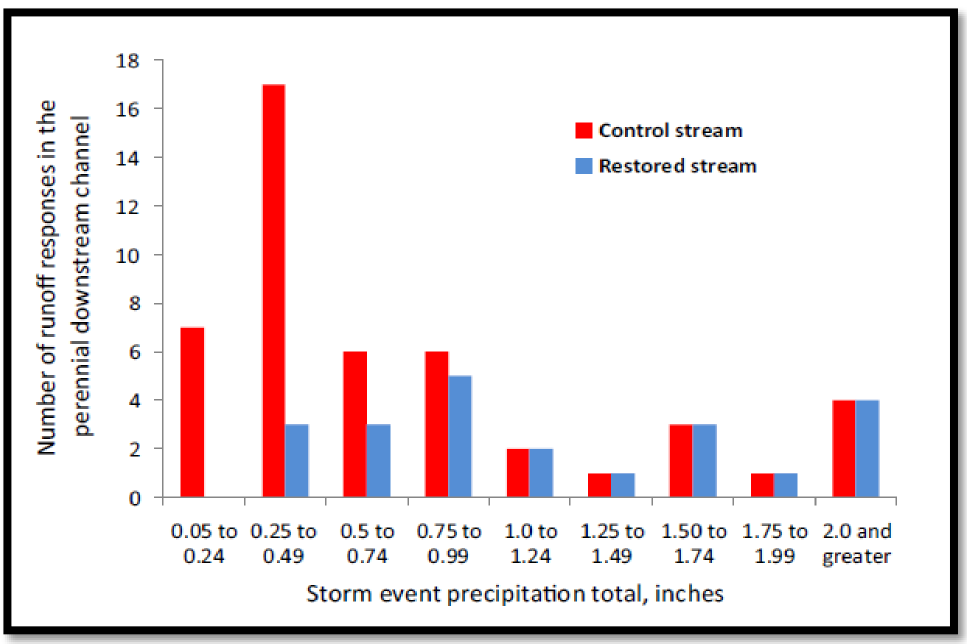

Figure 4: Runoff responses in restored and incised channel (Palmer et al. 2013)

b) The Problem

Stream restoration practices are increasingly being used for stormwater and erosion management, thus it is important to document whether they function as planned (Palmer and Allen, 2006). Because SPSC systems are a relatively new method of restoration, there are not many field data available on their performance. Studies such as Palmer et al. 2013 and an unpublished study by North Carolina State University (2014) have studied surface flow in these SPSC systems. For these systems to function as stormwater retention sites, however, they must be able to infiltrate and store stormwater or to store stormwater in surface pools There has not been little published research on infiltration, groundwater drainage, and subsurface storage processes in project that use this restoration design. The benefit of monitoring groundwater is that it will help determine if these systems have sufficient subsurface storage capacity to be viable options for stormwater retention and water quality remediation. SPSC systems are built with sand, gravel, and boulder-sized sediment, which should lead to high infiltration capacities and high hydraulic conductivities, but practitioners often infill with local soil during the construction process. Furthermore, fine-grained sediment washed from surface soils or roadways may clog pore spaces in the surface sediment. Therefore, the built SPSC system may have a different infiltration and storage capacity than planned

c) Hypothesis

H1: The infiltration capacity of these SPSC systems is based on the sand permeability, which is high. Therefore, stormwater retention limitations are due to storage limitations rather than limitations due to the infiltration capacity.

Null: Infiltration capacity is lower than expected for sand-sized grains, therefore, retention limitations can be due to infiltration capacity effects.

II) Method of Analysis

1) Field Methods

a) Measurement of Pool Surface Area

Surface area measurements were taken in all 16 of the pools in this system. Measurements were made with a tape measure anchored at one end by rebar. Length and width measurements were taken from several locations in each pool and averaged to obtain average length and width. These averages were multiplied together to obtain the surface area.

b) Infiltrometer Measurements

Infiltration rate is the vertical movement of water into the soil due to gravitational draining and soil suction. In order to determine the infiltration rates for sediment in the SPSC system, infiltration measurements were made in selected pools. Infiltration measurements can be made with different types of infiltrometers or permeameters. I used a single ring infiltrometer with a falling head test. A falling head infiltration measurement is when an infiltrometer is inserted into the soil and water is added to a given head, measurements of the water level are recorded at time intervals as the water infiltrates into the soil. From the change in water level and time, the amount of water that has been infiltrated into the soil can be calculated. (USGS 1963). I constructed a 12" diameter single ring infiltrometer out of low-gauge sheet metal (Figure 3). In the field, the infiltrometer was placed in the desired location and driven into the soil with a maul that hit a 4x4 piece of lumber placed over the ring. The 4x4 was equipped with a level to ensure vertical emplacement of the

Figure 5: Photograph of the infiltrometer test in the field

infiltrometer. The infiltrometer was driven 6 inches into the soil for each test. Water depth in the infiltrometer was measured with a tape measure fixed to the side of the infiltrometer to obtain water level changes.

c) Groundwater Well Installation and Head Measurement

Groundwater head data were used to determine subsurface storage capacity and drainage rate. These data are necessary to evaluate the potential for storm-water retention. Unsaturated zone storage potential requires data on water table elevations. Therefore, wells were installed in pools located throughout the SPSC system. The wells are composed of PVC pipe ranging from 1 ½" to ¾" in diameter that were slotted at depth and covered with fine nylon mesh to prevent sediment from entering the well. Caps were placed on both ends of the well to keep rain water from entering the top and sediment from entering the bottom. A vent hole was drilled into the side of the well near the top. The wells were installed by using an auger to make a hole in the soil. The well was then placed in the hole and then driven further into the ground with a maul. Head measurements are made by using a steel tape covered with mud (or chalk) and inserting it into the well. When it is removed, the depth at which the mud is removed accurately records the depth of water in the well, which can be converted to head (elevation) from knowing the elevation of the base or top of the well, This technique provides an accuracy of several mm and is not sensitive to changes in temperature or atmospheric pressure. Elevation of the water table is measured from the top of the well so that sedimentation will not affect the accuracy of the measurements. Each well was monitored on a weekly basis, and when possible, well elevations were measured prior to and after storm events. Selected wells were monitored with pressure transducers to determine ongoing time series data of water table elevations (Figure 6).

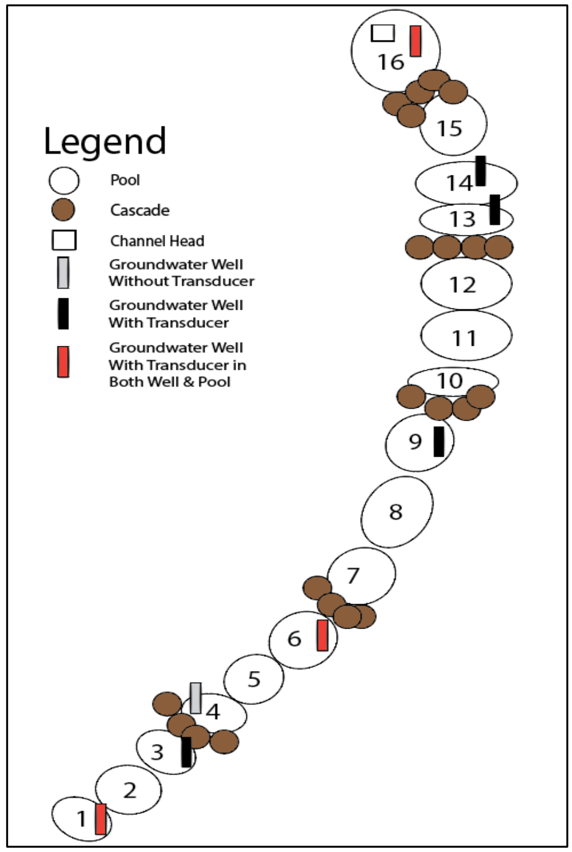

Figure 6: Sketch of the SPSC system at Carriage Hills


Figure 7: Well installed in pool 3


Figure 8: Onset HOBO data logger

d) Survey and Well Elevations

A longitudinal profile survey was completed for the restored stream. Starting from the base of the stream, elevation measurements were taken at 3 pool intervals (the major step height interval in the system). With the use of a string level and stadia rod, the change in height was recorded. This produced a total horizontal system length as well as a total elevation drop over the restored system. This allows for comparisons to be made between the ground surface elevation and the water table height. In addition to the longitudinal survey, several measurements were made on each well such as total length of the well, the amount exposed, and the screened interval. Sediment data and core samples were also taken during the well installation and the depth of permeable sediment was recorded. These measurements were used to identify the sediment that is at the screen interval depth.

e) Stratigraphy and Sediment Sampling

At each location where wells were installed, sediment samples were collected to study the characteristics of the soil. Having soil characteristics aided in determining grain size distribution, porosity and specific yield. As sediment was removed with the auger, sediment type such as organic matter, sand and clay at depth was recorded. From these data, we were able to make a hydrostratigraphic column and calculate the depth above clay or other low hydraulic conductivity layers. Sieve analysis was also done on samples to determine the grain size distribution in order to calculate hydraulic conductivity. The samples were weighed and then sieved through the stack.

2) Analytical Methods

a) Infiltration rates

The infiltration rate (IR) is calculated through a series of simple calculations. The area of the ring is calculated by finding the area of a circle $A=\pi r^2$. The next step is to determine the change in volume of water inside of the infiltrometer (Δ Volume= Volume $_{initial}$ – Volume $_{final}$). From knowing the area of the ring, the volume of water and the change in time, infiltration rate can be calculated using the infiltration rate equation (Erickson et al. 2010, Elrick, 1990, Seybold 2010)

$$q=Q/\pi r^2 t$$

where q= infiltration rate, Q= change in volume, r= radius of the ring, and t= time elapsed from first to last measurement.

b) Infiltration Volume

The field measurements of infiltration capacity can be combined with the measurements of pool area and the duration of pool saturation (time that the water table at or above the surface) to determine total infiltration volume for each pool and storm event

$$\mathbf{V\ (m^3) = I.R.\ (m/hr) * saturation\ time,\ hr * A\ (m)}$$

Where V= infiltration volume, I.R= infiltration rate and A= pool area.

c) Storage

With known ground elevation from the longitudinal survey and water table elevation with respect to time from well measurements, surface storage was calculated:

Available subsurface storage = (Ground elevation – w.t. elevation)*(n – Sr)

Where n= porosity and Sr= specific retention. This calculation produces the depth of available storage, m, which can be multiplied by pool surface area to determine available storage volumes. These calculations were made for each water table elevation, and thus produce time series data of available storage volume for each pool as a function of time.

d) Hydraulic Conductivity

From the data obtained from the sieve analysis, hydraulic conductivity was calculated for the selected samples.

$$\mathbf{K=1300\ [I_0 + 0.025\ (d_{50} - d_{10})]^2}$$

Grain size analysis results were plotted on a graph in Microsoft excel. From the graph, the variables I_0 = the intercept of the trend line on the horizontal axis, d_{50} = the median grain size, or the value of the sediment diameter for 50% of the cumulative distribution and d_{10} = the value of the sediment diameter for 10% of the cumulative distribution were calculated to determine the hydraulic conductivity (Alyamani, M. S. and Şen, Z., 1993).

III) Results

1) Site Characteristics

The width and depth of each pool in the system was measured to obtain the pool surface area. A schematic diagram of the pool arrangement is shown in fig. 5 (and appendix). Each pool was installed as a series of 3 pools, with the major elevation drop at the third pool in each series.

The sites of elevation drops are armored with boulders to prevent erosion (fig. 5). The average pool width is 18.4 ft (5.61 m), the average pool length is 24.27 ft (7.52m) and the average pool area is 438.9 ft^2 (40.78 m^2). Data obtained from the longitudinal survey indicate that the total elevation change from head to toe of the restoration feature was 12.37 m and the step-pool system has a total length of 115.3 m, thus giving an average gradient of 0.108 for the system. This gradient has been broken into sequences with much lower gradients, separated by 5 major steps. The average height of each step is 2.74 m, but the step height is not distributed equally, the step height at the downstream end of the system is significantly higher than the other steps.

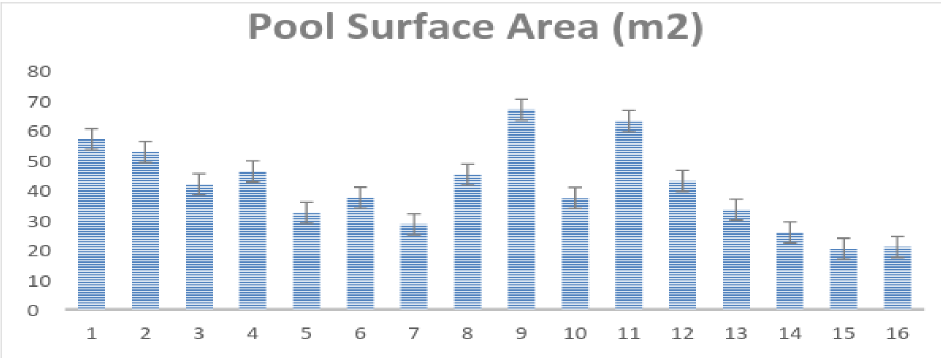

Figure 9: Graph of pool surface area distribution

The longitudinal distribution of pool areas is shown in fig. 8. The pools have similar areas. The pool areas are largest in the middle of the system, which also had the shortest step heights. Largest step heights and smallest pools are located at the downstream end of the system. Sediment samples were also collected in selected pools throughout the system with the use of a soil auger. Soil characteristics were noted at various depths. The depth to the clay layer is shown in fig. 9. This measurement shows how groundwater will probably flow through layers of different hydraulic conductivities.

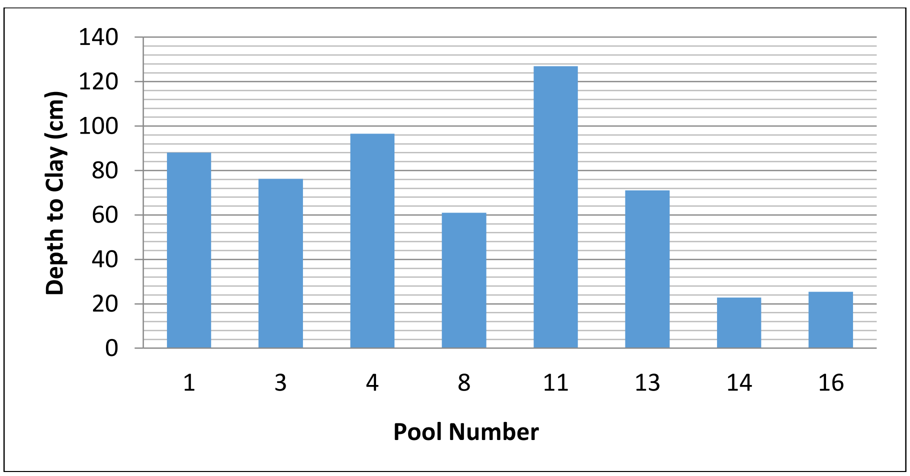

Figure 10: Depth below the surface to the clay layer

2) Infiltration rates

Infiltration measurements were taken in four pools within the restored stream (Pools #16, 13, 8 and 4). These 4 pools were chosen because they were spaced out throughout the system and their beds did not contain a large amount of cobbles in the beds, which facilitated the infiltration measurements. In each chosen pool I conducted three infiltration tests in different parts of the pool to account for surface heterogeneities and to calculate infiltration variance.

Table 1: Mean infiltration, variance and standard deviation for the four infiltration tests

Site	Pool 16	Pool 13	Pool 8	Pool 4
Mean infiltration rate, cm/hr	8.5E-03	1.3E-02	9.1E-03	2.0E-02
Variance, cm/hr	8.5E-07	3.7E-05	1.4E-05	3.4E-06
Standard deviation, cm/hr	9.2E-04	6.0E-03	3.7E-03	1.8E-03

Table #1 shows the average results from the three infiltration tests in each selected pool. These data suggest that there is a difference in infiltration rate within a single pool; therefore multiple tests are necessary to account for bed heterogeneities. Trials #1 and #3 were taken at the edges of the pools whereas trial #2 was taken in the middle of each pool where the flow is concentrated during storm events. This difference could be due to saturation which inhibits infiltration, or by some erosion of the sandy bed making the surface closer the lower infiltration clay. As a whole these infiltration rates seem low for a pool filled with a sandy sediment (Messing 2005). Examination of the surface sediment suggests that the settling of fine material in the pools may have significantly lowered pool infiltration capacity. Infiltration rates for pools 16, 13, 8 and 4 can be found in the appendix.

Total infiltration volume was also calculated for events in which enough stormwater entered the system to create ponding in the pools. The graph below shows the ponding depth and duration for pool 16 during the rain event that occurred between 10/1/15 and 10/3/15. These data were collected from the data logger that was placed on the surface of the pool.

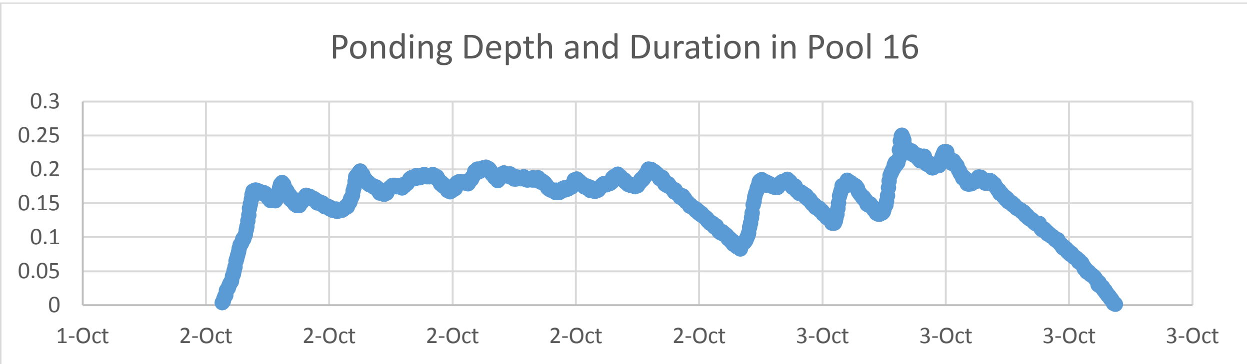

Figure 11: Time series of ponding depth for pool 16

From these data the total duration of ponding was found to be 33 hours and 28 minutes. When using the equation $V(m^3)$ = I.R. (m/hr) * saturation time, hr * A (m), the total infiltrated volume is 162 m^3.

3) Seasonal changes in Groundwater Head

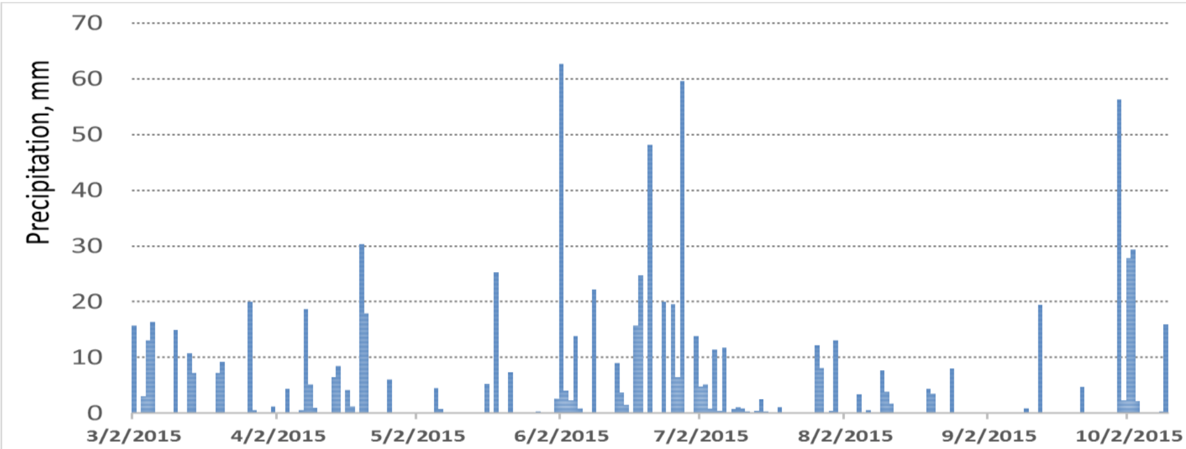

Figure 12: Precipitation data at the study site during the monitoring period

Above is the precipitation data from the study site during the monitoring period of this research. Spring of 2015 consisted of regular precipitation events of moderate magnitude with an average storm producing about 10mm of precipitation. This was followed by a wet early summer, with five precipitation events producing more than 20mm of precipitation. Late summer into early fall was dry with very little precipitation with only one storm with significant precipitation that occurred in early October. This pattern of precipitation, produced high water tables in the early spring that declined through most of the summer period.

Seasonal differences in water table elevation are observed in the longitudinal profiles. These graphs below represent the seasonal variations that occur for the system as a whole. In the wetter spring months, the water table was much closer to the surface and had more variance in depth between the different pools. Leading into early summer when there was a decline in precipitation, the water table level dropped significantly below the ground surface. There could be several causes for this difference in groundwater behavior. The most apparent possibility is that in early spring, the groundwater was influenced by snow melt and a greater amount of precipitation. Another possibility is that in early summer evapotranspiration begins to increase. In the cold months, the plants die back and have little effect on groundwater processes. In the spring and summer months however, the vegetation grows back and begins using the available water. There were significant precipitation events between 6/1/15 and 7/15/15 which is show in figure 12. However, even during this period of stormy events, the water table continues to decline. The probable cause for this decline in water table is evapotranspiration.

Figure 13: Photograph showing little vegetation in winter months

Figure 14: Photograph showing live vegetation in late summer

Figures 13 & 14 show the difference in vegetation in the system during different times of the year. In the winter and early spring, vegetation is dormant. The lack of transpiration from the plants prevents groundwater from being used and promotes infiltration and storage. From late spring and into the summer months, the vegetation grew back. Water table elevation measurements showed there was more storage present in the system during months when vegetation was thriving, suggesting evapotranspiration aids in the availability of groundwater storage (Figure 15).

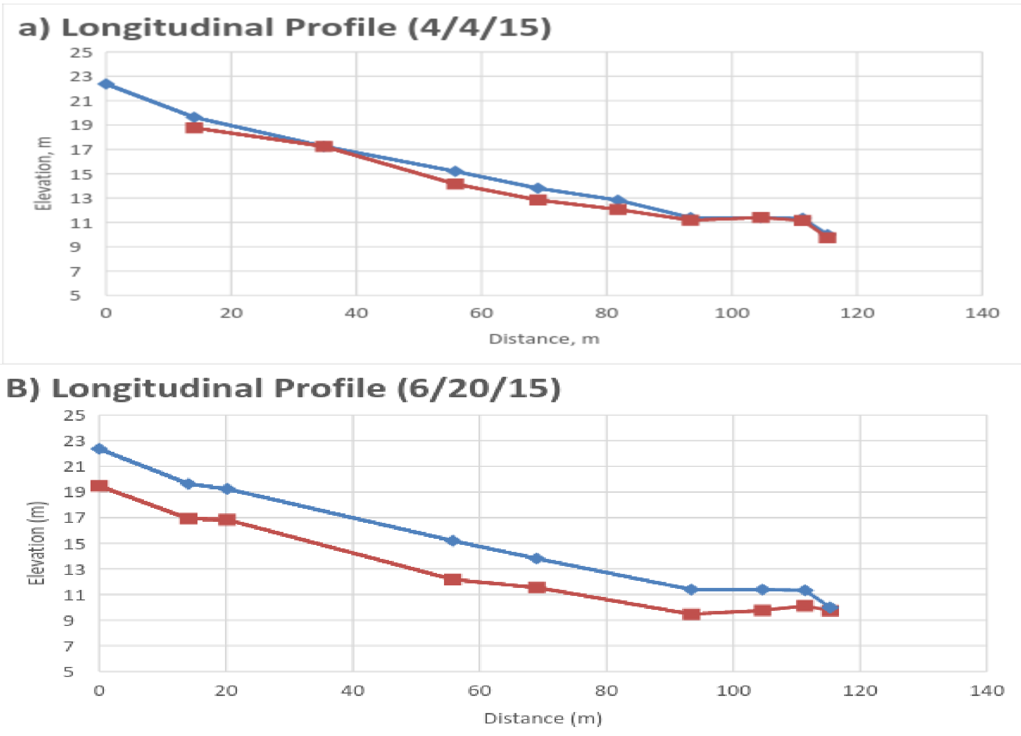

Figure 15: Graphs a and b show the distance from the ground surface to the water table for late winter and early summer

Water table measurements were taken using biweekly measurements and continuous monitoring at 2 minute intervals with pressure transducer and data loggers. From March through September, only biweekly measurements were taken. Due to the longer intervals between measurements, these data are used to show seasonal variations in the groundwater levels. Examples of water levels for the time period are shown in figure 16 (a-d), which illustrate water level changes at the head, middle, and toe of the step-pool system.

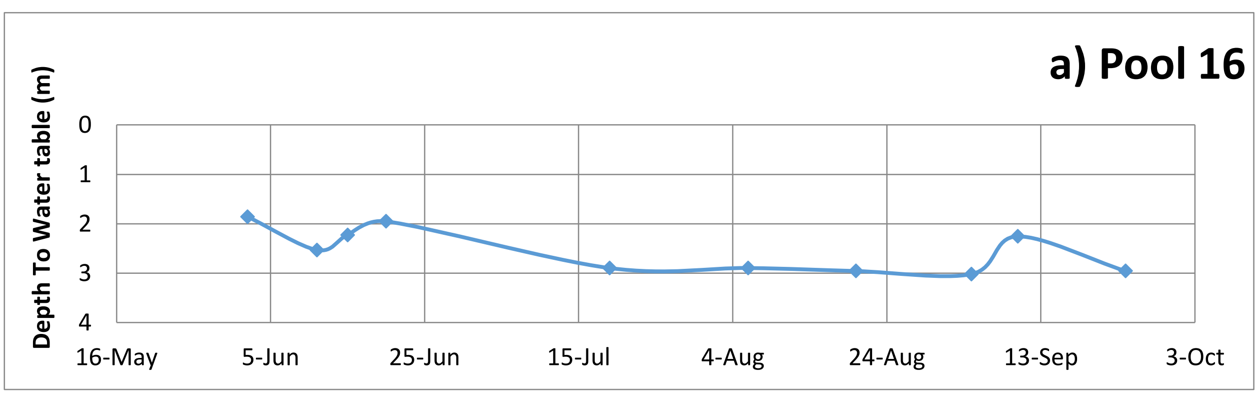

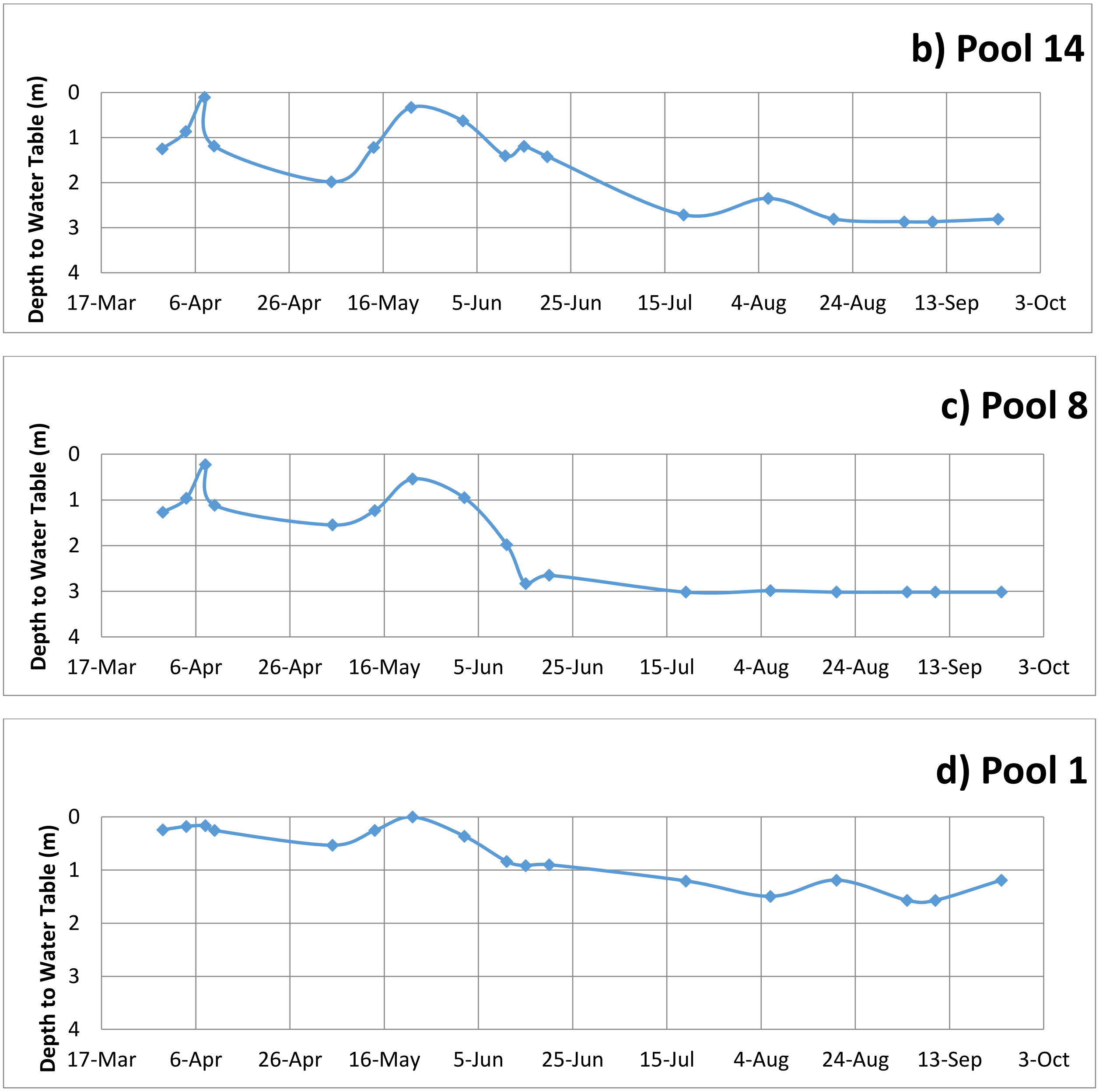

Figure 16: Depth to Watertable for pools from upslope to downslope locations

These graphs represent the change in water table elevation over a six month period. The depth to the water table is greatest at the head of the system, Pool 16. Water table under pools in the middle of the system were shallow during rainy periods but dropped to greater than 2 m depth during dry periods. Pool 1, which is located at the end of the system, exhibits the shallowest water table, and a more gradual peak and recession than upstream pools. The reason for this is that as the groundwater is flowing laterally down the system, the drainage from the previous pool flows down through the subsurface area of the subsequent pools. Pool 14 is closer to the head of the system and there are only two pools that contribute to the recharge. Pool 16, at the head of the system has no lip to the edge of the pool, and therefore does not pond water during storm events. Pool 16, however, receives all the runoff from the storm sewer system, thus it also illustrates the response of the groundwater at a pool site where ponding is not occurring during storm events.

4) Storm-induced changes in water level during the fall recharge period

Data loggers were installed at the end of September in order to see the changes in groundwater storage that occurred over the course of individual storms. Data was collected at two minute intervals. These data collected from the loggers have shown a more intensive view of the subsurface behavior in response to storms after a prolonged dry period. In the graph below, the depth from the ground surface to the water level is plotted over time. The early October storms occurred after a long dry period. The data logger registered no groundwater in the well until the large precipitation event in early October. From the two minute interval records of pressure and temperature, the elevation was calculated. This data series helps depict many factors of groundwater flow that was not visible from the previous biweekly measurements such as the rising and recession limbs. In pool 16, the receding limb shows a steep slope of drainage to around 1.1m and then proceeds to drain at a slower rate. This may be due to the water passing through the sandy layers that have higher infiltration rates down into the lower infiltration rate sediments at depth.

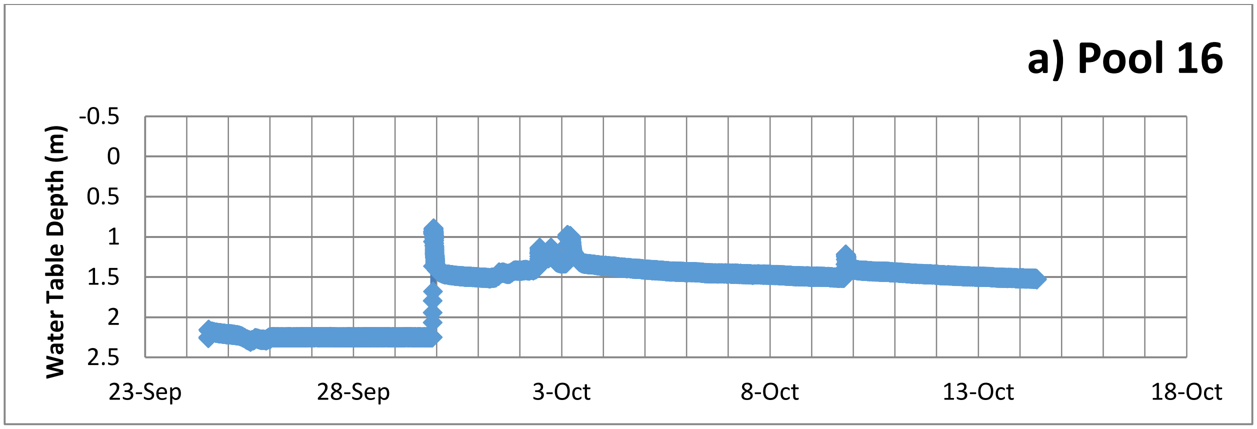

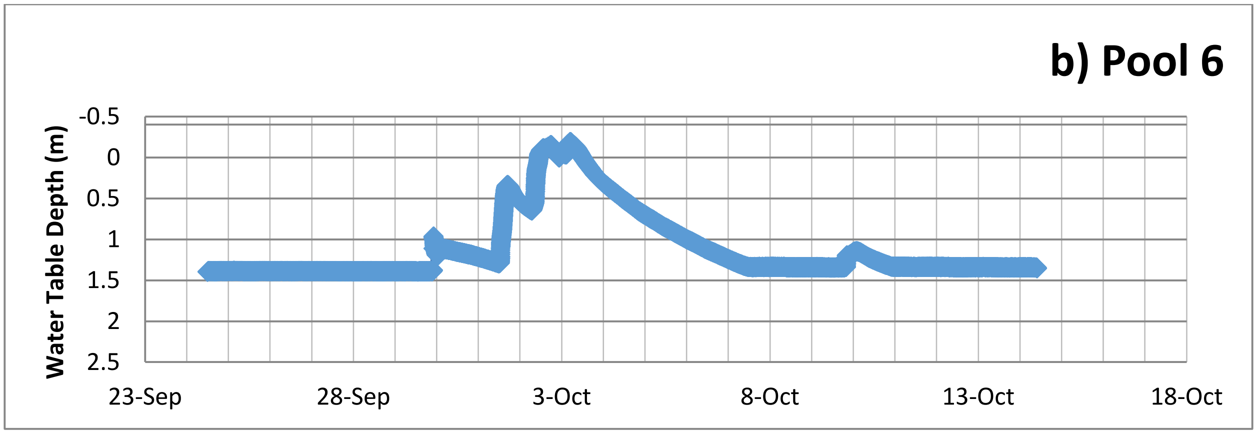

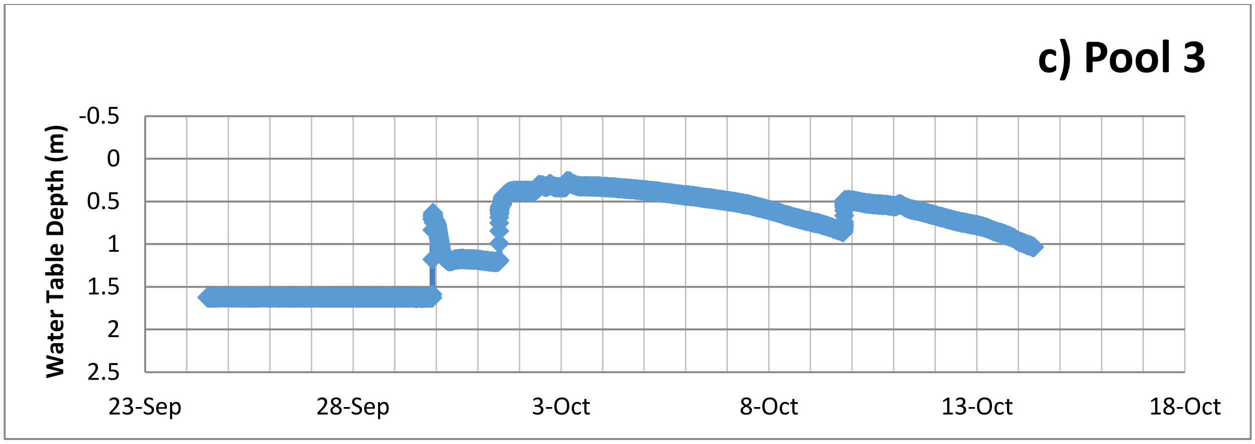

Figure 17: Response of water table to storm events.

Groundwater responses due to storm events vary from upslope to downslope in this restoration. In pool 16 there was a rapid increase followed by a rapid decrease in water table elevation caused by the influx of water brought into the system though the stormwater drain. The prolonged dry period before this rain event allowed for rapid drainage downslope.

Pools downslope from the head show a similar rise in water table elevation at the onset of a storm event, however they have more gradual recession limbs. Pool 6 shows a cumulative increase in elevation as the precipitation and runoff accumulates. When the precipitation concluded, the water table receded 1.6m in about 5 days. Pool 3 exhibits the most gradual recession of water table elevation of 0.6m in the same time period.

5) Grain Size Analysis and Hydraulic Conductivity Estimates

Grain size distribution was measured for surface sediment in pools 8 and 14, in addition to sediment at a depth of 8”-24” in pool 8. These values were averaged to get an estimated grain size distribution for the whole system

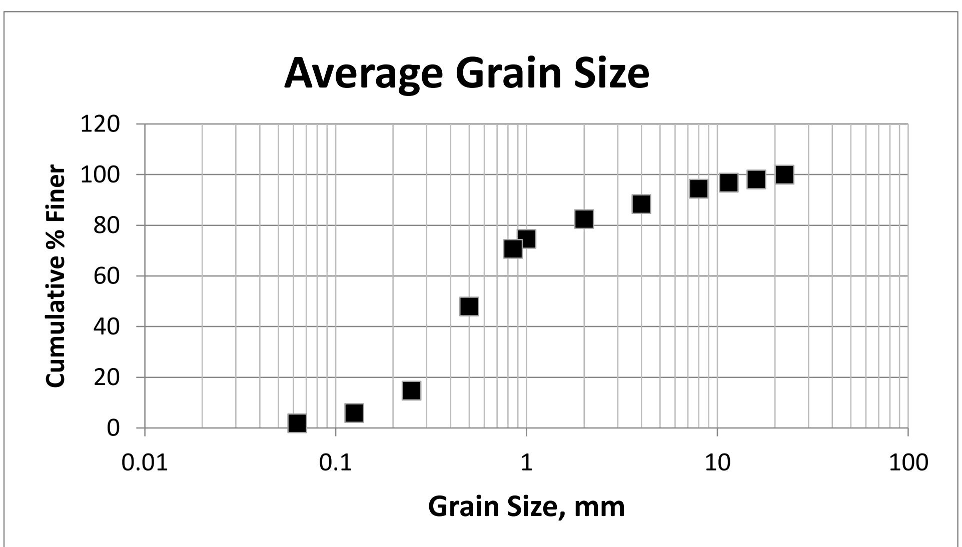

Figure 18: Average grain size distribution

Table 2: Averaged results from the sieve analysis

size, mm	weight, g	WT %	cum % finer
32			
22.5			100
16	3.07	1.87	98.13
11.5	1.97	1.20	96.93
8	4.00	2.44	94.49
4	10.07	6.14	88.36
2	9.60	5.85	82.51
1	12.93	7.88	74.62
0.85	6.47	3.94	70.68
0.5	37.13	22.63	48.05
0.25	54.63	33.30	14.75
0.125	14.40	8.78	5.97
0.063	6.77	4.12	1.85
0.03	3.03	1.85	

The sieve analysis shows that the average, D_{50}, grain size for this system is 0.594 and a D10 grain size of 0.159. There is also evidence of finer particles being deposited on the surface because one third of the sampled sediment has a grain size between 0.25 and 0.5 mm.

These data allowed for estimates to be made for hydraulic conductivity (K). Figure 19 shows a graph of the grain size distribution for grains less than 0.85mm in diameter. The reason for using smaller diameter grains to determine the hydraulic conductivity is that smaller grains have a greater effect on K values than larger grains (Alyamani, M. S. and Şen, Z., 1993).

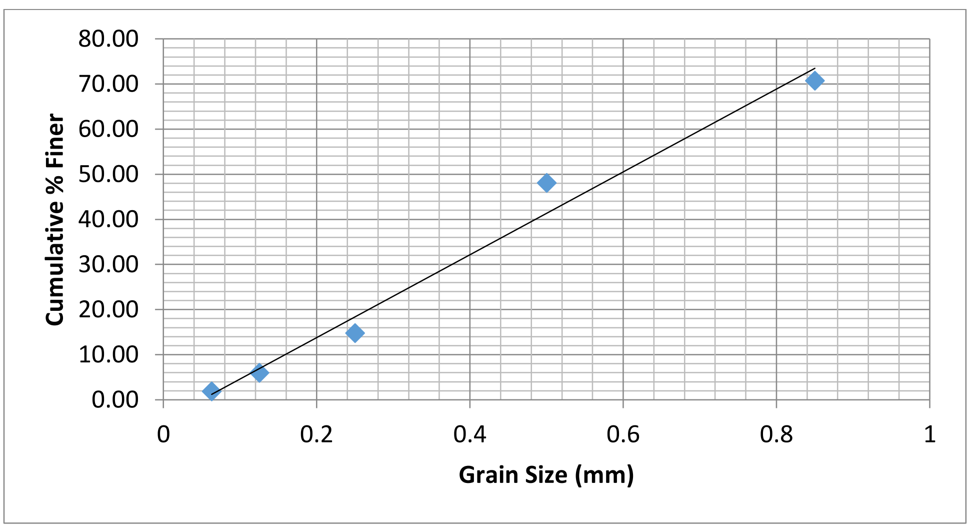

Figure 19: Grain size distribution for smaller diameter grains

Table 3: Calculation of average hydraulic conductivity

I_0	D_{10}	D_{50}	D_{50}-D_{10}	.025* D_{50}-D_{10}	(.025* D_{50}-D_{10})^2	K m/day	K m/sec
0.0498	0.1587	0.5943	0.4356	0.0109	3.69E-03	4.7920	5.55E-05

The calculated hydraulic conductivity for this system is 5.55E-05 m/sec which is within the accepted value for a fine grained sand (Domenico and Schwartz, 1990).

6) Storage

The storage for this system was calculated in order to determine if this restoration is storage or infiltration limited. In order to calculate the storage, the porosity and specific retention were determined based on results from the grain size analysis. Using the D50 grain size, the specific retention was estimated to be 0.09 (figure 20) and the porosity to be 0.35 (Beard and Weyl 1973).

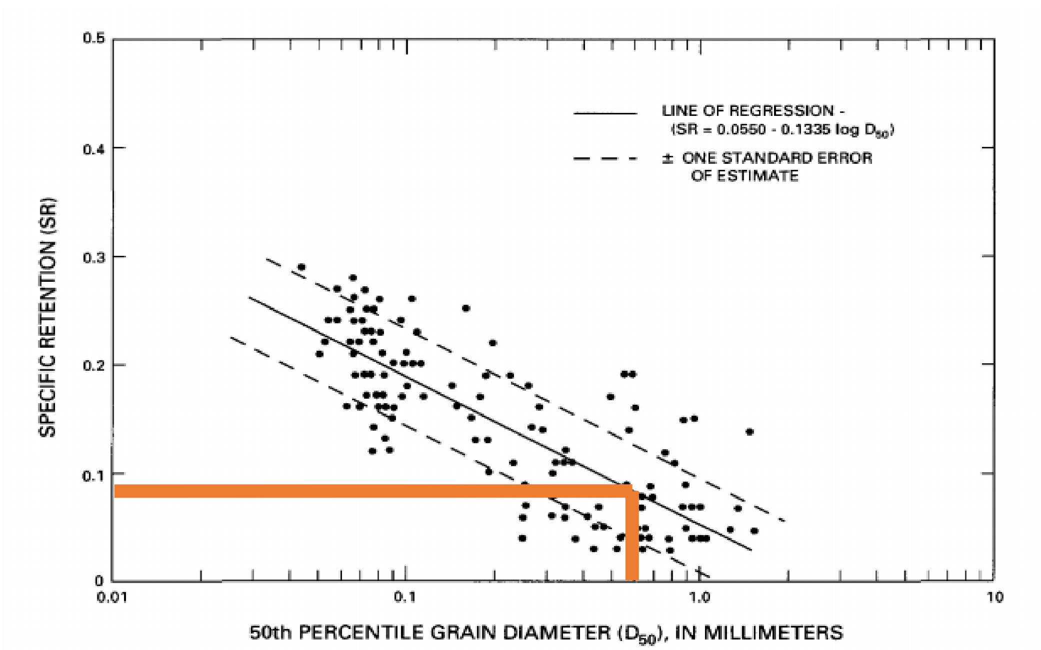

Figure 20: Specific retention estimates from D50 (USGS 1993)

Combining the data that was collected; storage depth, storage volume and total system storage was calculated. Seasonal variances can be seen below. In early spring, when there was significant precipitation and a low amount of evapotranspiration, there was very little storage available in the system. In early summer, when there were multiple large magnitude storms, there is more storage space available most likely due to evapotranspiration. Finally in late summer and into early fall, lower amounts of precipitation combined with the effects of evapotranspiration, there was a greater amount of storage space available.

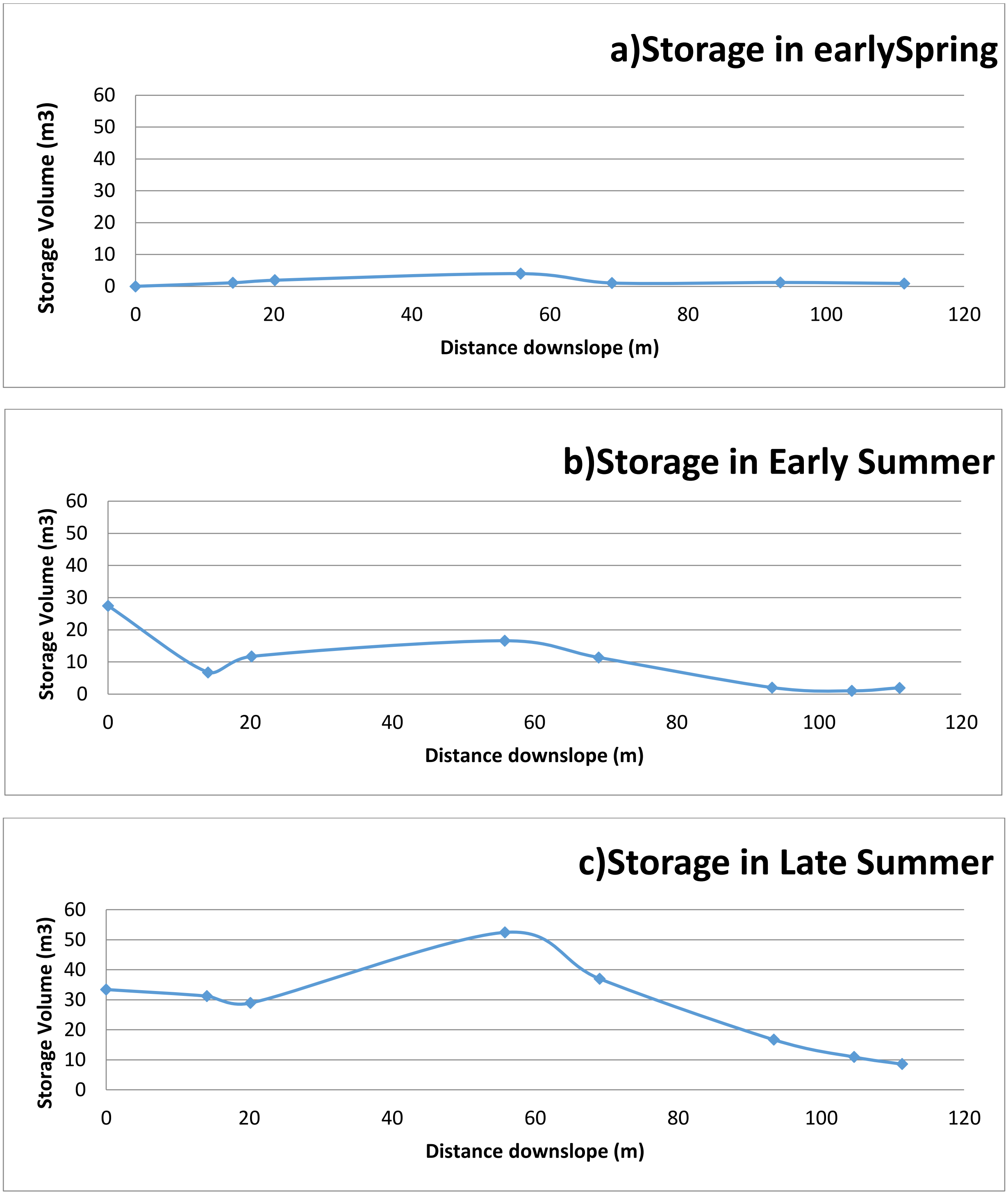

Figure 21: Changes in storage volume in various seasons

Table 4: Seasonal varience in storage volume for this SPSC system

Pool #	16	14	13	8	6	4	3	1
Water Table elevation (m) 4/8/15	NA	0.102	0.159	0.229	0.064	0.140	NA	0.165
Storage Depth (n-S_R)* m	NA	0.026	0.041	0.059	0.017	0.036	NA	0.043
Pool Area (m2)	56.961	41.897	46.192	66.859	63.075	33.388	25.76341	20.942
Storage Volume (m3)	NA	1.107	1.907	3.974	1.041	1.213	NA	0.899

Pool #	16	14	13	8	6	4	3	1
Water Table elevation (m) 6/2/15	1.856	0.624	0.975	0.955	0.695	0.236	0.152	0.362
Storage Depth (n-S_R)* m	0.483	0.162	0.254	0.248	0.181	0.061	0.040	0.094
Pool Area (m2)	56.961	41.897	46.192	66.859	63.075	33.388	25.763	20.942
Storage Volume (m3)	27.487	6.793	11.712	16.603	11.399	2.050	1.020	1.971

Pool #	16	14	13	8	6	4	3	1
Water Table elevation (m) 9/10/15	2.256	2.865	2.408	3.018	2.256	1.920	1.631	1.570
Storage Depth (n-S_R)* m	0.586	0.745	0.626	0.785	0.586	0.499	0.424	0.408
Pool Area (m2)	56.961	41.897	46.192	66.859	63.075	33.388	25.763	20.942
Storage Volume (m3)	33.404	31.211	28.919	52.455	36.990	16.669	10.923	8.547

7) Discussion of Uncertainty

For all scientific measurements there is some amount of error present. For my research, the error will come from sampling disturbance and the tools used to determine infiltration rate, water table elevation and the longitudinal profile. When procedures such as infiltration tests and well installation occur, there is some degree of ground disturbance that can affect the measurements. These disturbances are sources of error in the data. Also, when using measuring instruments there is a certain level of accuracy to which they can measure. For these measurements, a tape measure or a stadia rod was used. For the tape measure, the uncertainty is ± $^{1}/_{16}$” or 0.159 cm. For the stadia rod, the uncertainty is 0.5 cm. For the data loggers that were used for pressure readings, the manufacturer states that for pressure, there is a maximum error of 0.62 kPa and for water level measurements, there is a maximum error of less than 1cm.

IV) Discussion and Conclusions

Step Pool Stormwater Conveyance Systems are beneficial in many ways for stream restoration. Fortifying the stream bed with a series of large boulders has kept headward erosion and channel incision from occurring. However the use of sand in the bases of the pools may not be promoting infiltration the way they were engineered to. From the results obtained from the infiltration tests, the surface does not have a high infiltration rate. Small particles have settled onto the surface and decreased the infiltration capacity in the pools.

However, even with a low infiltration rate measured in many of the pools, when there was a storm of significant magnitude, ponding times in the pools was significant, allowing for significant infiltration. The water table reached the surface in two of the pools that were monitored with wells during fall storm events. In the two pools that exhibited an above-surface water table, the surface ponding duration was significantly longer than the time the head elevation was above ground level. This indicates vertical gradients in head and also suggests that infiltration rate at the surface is slower than the drainage rate at depth. Surface infiltration could be limited by fine-grained sediment deposited in the pore spaces of the coarse sediment.

The upper pools were not saturated to the surface during storm events and had very low water tables during the dry summer months. Most of the storage capacity of the system is in these upper pools. The time series data during storms, however, indicates that much of this storage capacity is not utilized. This suggests that the upper portion of the system is infiltration-limited, whereas the lower portion is saturated more of the year and these pools are storage-limited.

a) Suggestions for Future Work

For future work, continual monitoring of the sites with the use of pressure transducers will help get a better understanding on seasonal responses to groundwater flow. With more data points present in the spring and summer months, a greater understanding of evapotranspirative processes can be achieved. Infiltration and grain size analysis tests can also be conducted for the remaining pools in the system to get an even more in depth understanding of this restoration method.

V) Acknowledgments

I would like to thank Dr. Prestegaard for helping me from designing this project all the way through completing my final report. Her support and guidance has been vital in helping me get a better understating of geomorphic and groundwater processes. I would also like to thank Rosemary Fanelli for helping me with data collection and analysis, as well as answering all of my questions throughout this project.

VI) References

Alyamani, M. S. and Şen, Z. (1993), Determination of Hydraulic Conductivity from Complete Grain-Size Distribution Curves. Groundwater, 31: 551–555. doi: 10.1111/j.1745-6584.1993.tb00587.x

Beard, D. C. and Weyl, P. K.: "Influence of Texture on Porosity and Permeability of U nconsolidated Sand," AAPG Bull., Vol. 57, No. 2, (1973), 349-369.

Bouwer, H., & Rice, R. C. (June 01, 1976). A slug test for determining hydraulic conductivity of unconfined aquifers with completely or partially penetrating wells. *Water Resources Research, 12,* 3, 423-428.

Chin, A., & Wohl, E. (September 01, 2005). Toward a theory for step pools in stream channels. Progress in Physical Geography, 29, 3, 275-296.

Domenico, P.A. and F.W. Schwartz, 1990. *Physical and Chemical Hydrogeology*, John Wiley & Sons, New York, 824 p.

Erickson, A. J., Gulliver, J. S., Kang, J.-H., Weiss, P. T., & Wilson, C. B. (December 01, 2010). Maintenance for Stormwater Treatment Practices. *Journal of Contemporary Water Research & Education, 146,* 1, 75-82.

Elrick, D. E., Reynolds, W. D., Geering, H. R., & Tan, K.-A. (April 01, 1990). Estimating steady infiltration rate times for infiltrometers and permeameters. *Water Resources Research, 26,* 4, 759-769.

Hammer, T. R. (December 01, 1972). Stream channel enlargement due to urbanization.Water Resources Research, 8, 6, 1530-1540.

Hancock, G. R., & Evans, K. G. (September 30, 2010). Gully, channel and hillslope erosion - an assessment for a traditionally managed catchment. *Earth Surface Processes and Landforms, 35,* 12, 1468-1479.

Hazen, Allen. (1892) Some physical properties of sands and gravels: Massachusetts State Board of Health, Ann. Rept. pp. 539-556

Kuo, J. (2014). *Practical design calculations for groundwater and soil remediation*(Second edition.). Boca Raton, FL: CRC Press.

Leopold, L. B. (1968). *Hydrology for urban land planning: A guidebook on the hydrologic effects of urban land use*. Washington, D.C: U.S. Geolgoical Survey.

Messing, I., Iwald, J., Lindgren, D., Lindgren, K., Nguyen, L., & Hai, T. S. (September 01, 2005). Using pore sizes as described in soil profile descriptions to estimate infiltration rate and saturated hydraulic conductivity. Soil Use and Management, 21, 3, 276-277.

Montgomery, D. R., & Dietrich, W. E. (November 17, 1988). Where do channels begin?.*Nature, 336,* 6196, 232-234.

North Carolina State University (June 2014). Regenerative Stormwater Conveyance

http://www.bae.ncsu.edu/stormwater/training/ppts/rsc-intro_for_web.pdf

Palmer, M. A., Filoso, S., & Fanelli, R. M. (January 01, 2014). From ecosystems to ecosystem services: Stream restoration as ecological engineering. Ecological Engineering, 65, 62- 70.

Palmer, M. A., & Allan, J. D. (January 01, 2006). Restoring Rivers - The work has begun, but we have yet to determine what works best. Issues in Science and Technology, 22, 2, 40.

Paul, M. J., & Meyer, J. L. (January 01, 2001). STREAMS IN THE URBAN LANDSCAPE. *Annual Review of Ecology and Systematics, 32*, 333-366.

Sageev, A. (August 01, 1986). Slug Test Analysis. Water Resources Research, 22, 8, 1323-1333.

Seybold, C. (August 31, 2010). Single ring constant head infiltrometer. ftp://ftp-fc.sc.egov.usda.gov/NSSC/training/Soil_Tech_Measurement_and_Data_Eval/UNL_Field_Trip/Single%20ring%20infiltrometer.pdf

United States Geological Survey (1963) A field method for measurement of infiltration: Geological Survey water-supply paper 1544-H

Wilcox, A. C., Nelson, J. M., & Wohl, E. E. (May 01, 2006). Flow resistance dynamics in step-pool channels: 2. Partitioning between grain, spill, and woody debris resistance. Water Resources Research, 42, 5.)

Yu, G., Wang, Z.-Y., Zhang, K., Duan, X., & Chang, T.-C. (April 01, 2010). Restoration of an incised mountain stream using artificial step-pool system. Journal of Hydraulic Research, 48, 2, 178-187

VI) Appendix

1) Seasonal Water Table Measurements

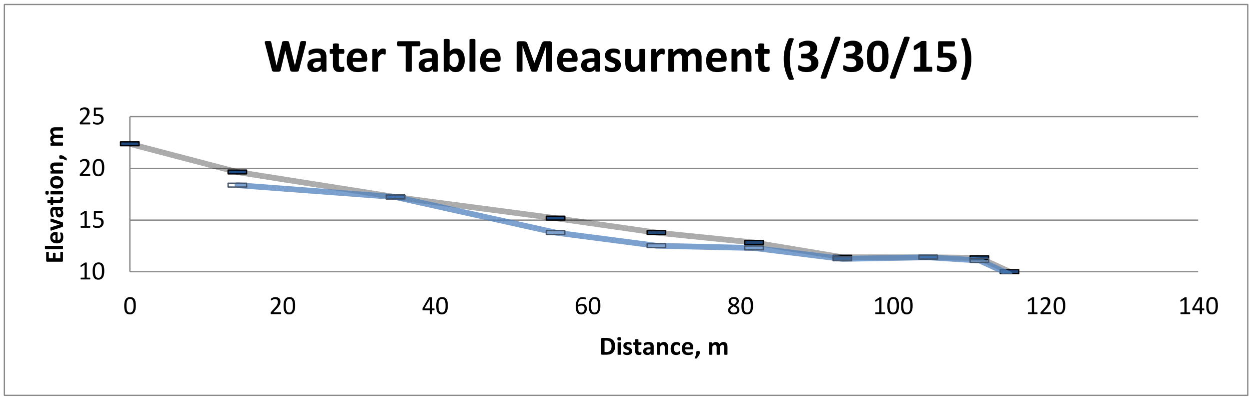

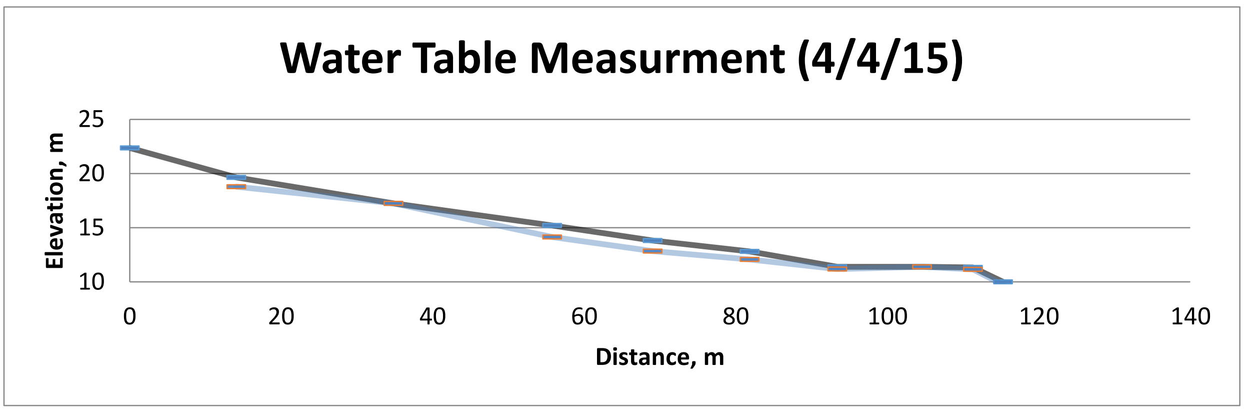

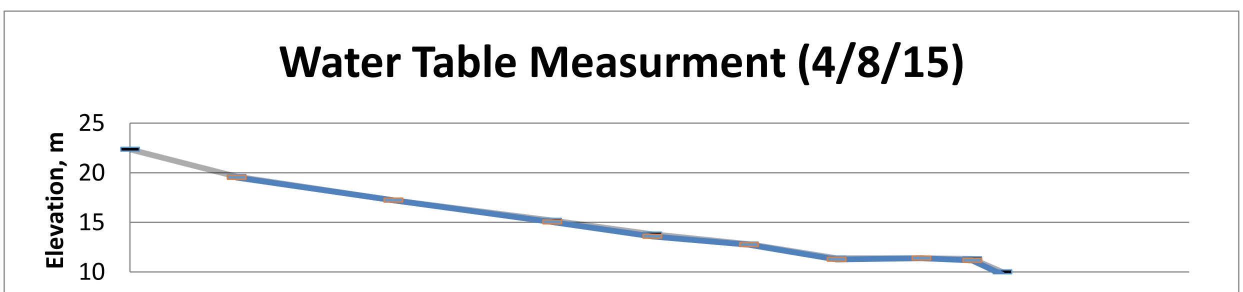

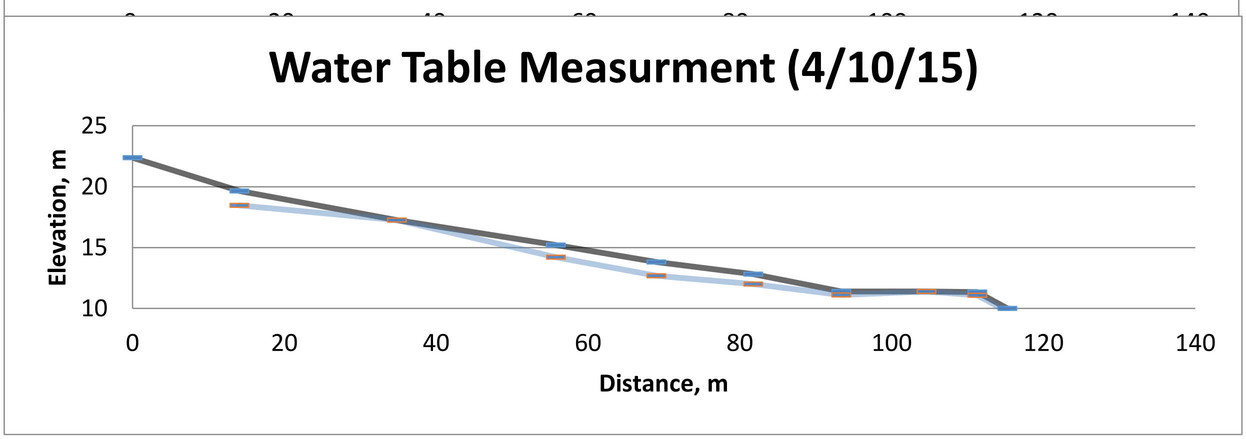

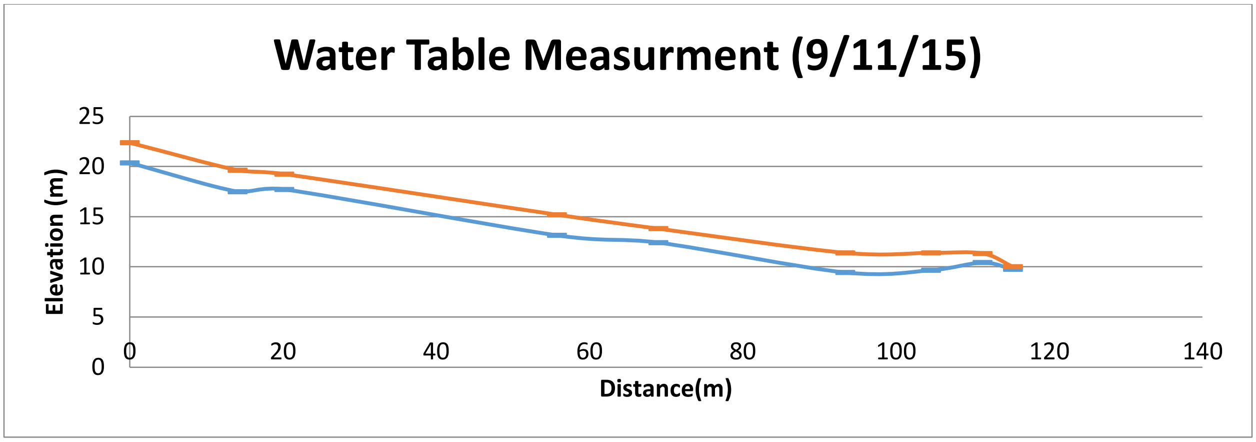
Water Table Measurment (9/11/15)
Elevation (m)
25
20
15
10
5
0
0
20
40
60
80
100
120
140
Distance(m)

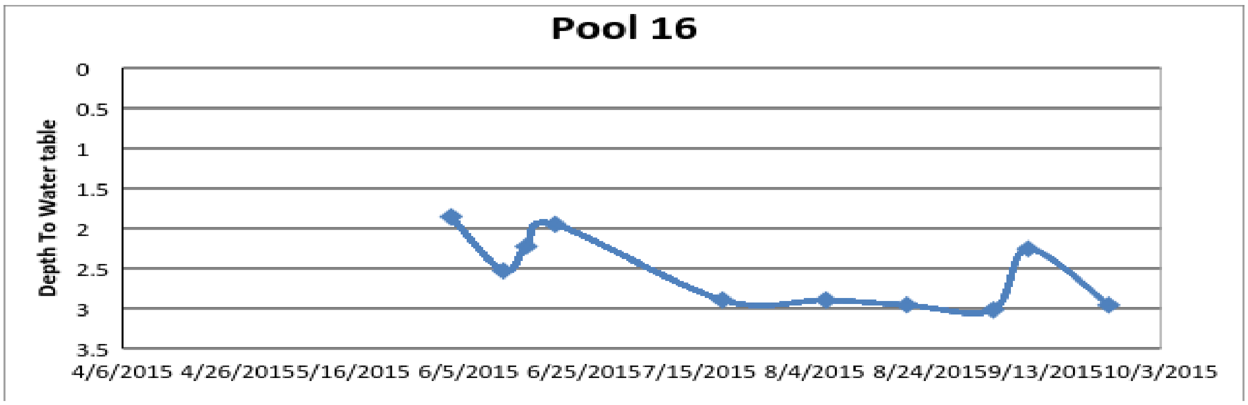
Pool 16
Depth To Water table
0
0.5
1
1.5
2
2.5
3
3.5
4/6/2015 4/26/20155/16/2015 6/5/2015 6/25/20157/15/2015 8/4/2015 8/24/20159/13/201510/3/2015

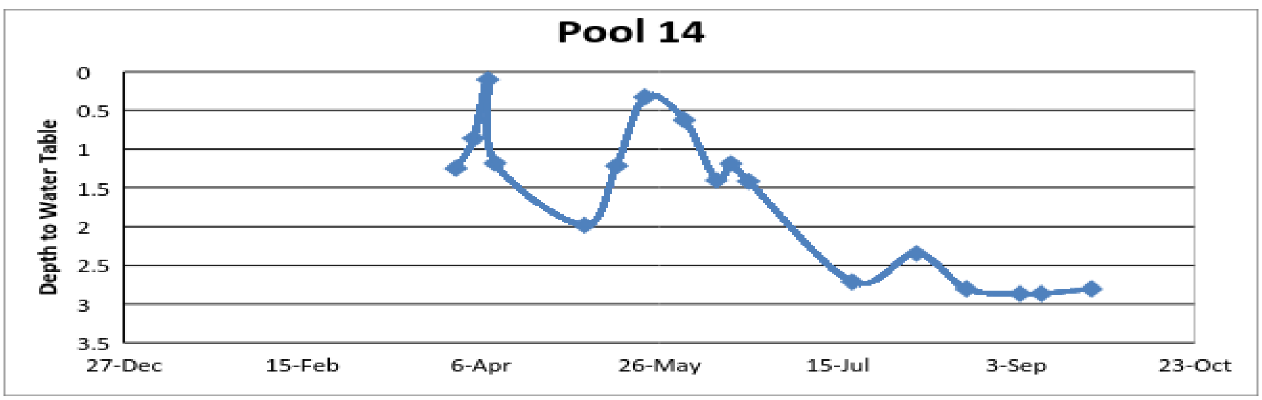
Pool 14
Depth to Water Table
0
0.5
1
1.5
2
2.5
3
3.5
27-Dec
15-Feb
6-Apr
26-May
15-Jul
3-Sep
23-Oct

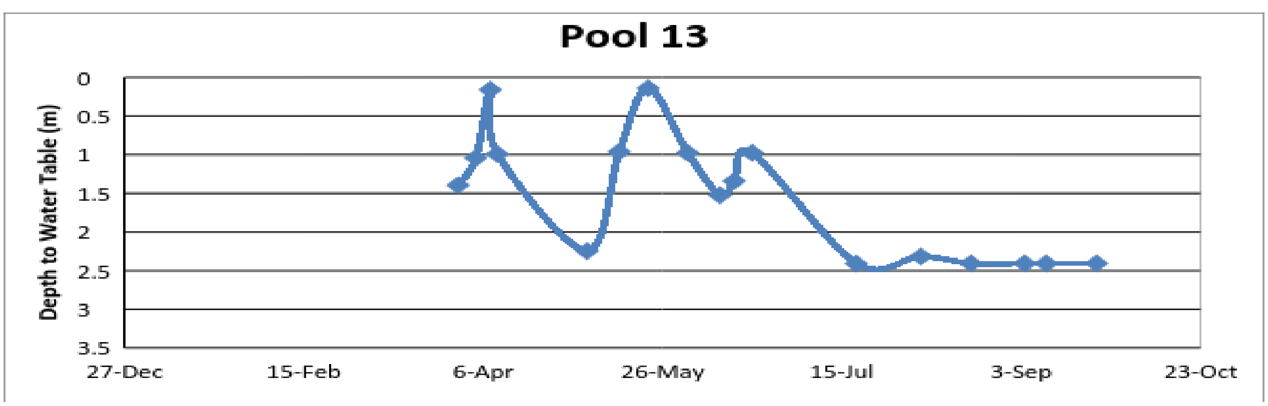
Pool 13
Depth to Water Table (m)
0
0.5
1
1.5
2
2.5
3
3.5
27-Dec
15-Feb
6-Apr
26-May
15-Jul
3-Sep
23-Oct

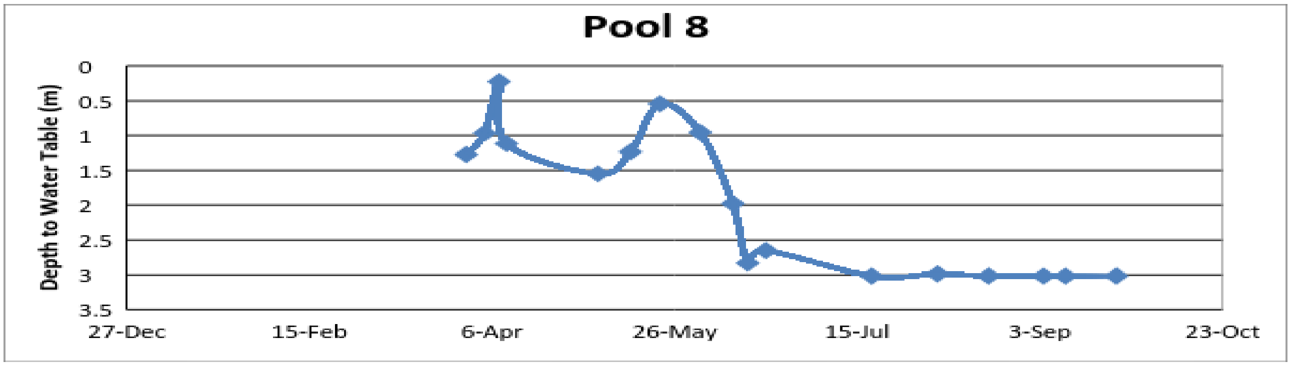
Pool 8
Depth to Water Table (m)
0
0.5
1
1.5
2
2.5
3
3.5
27-Dec
15-Feb
6-Apr
26-May
15-Jul
3-Sep
23-Oct

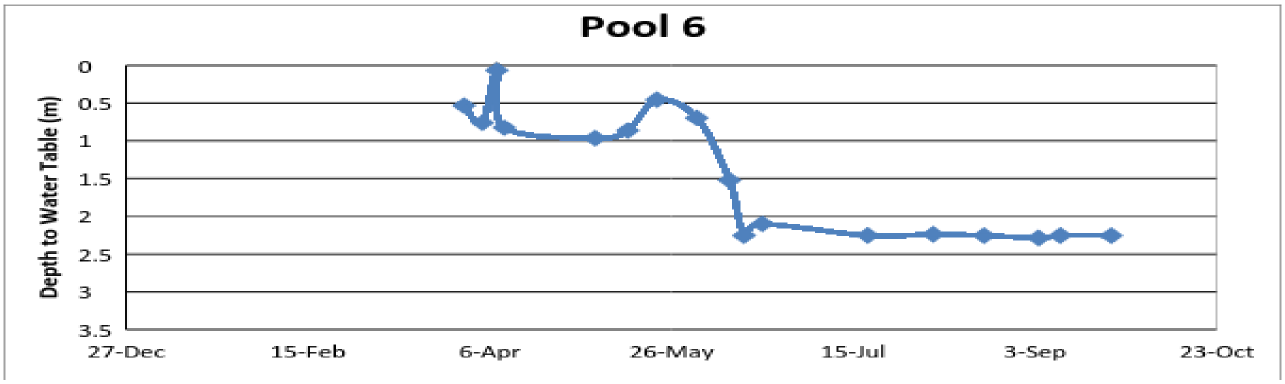
Pool 6
Depth to Water Table (m)
0
0.5
1
1.5
2
2.5
3
3.5
27-Dec
15-Feb
6-Apr
26-May
15-Jul
3-Sep
23-Oct

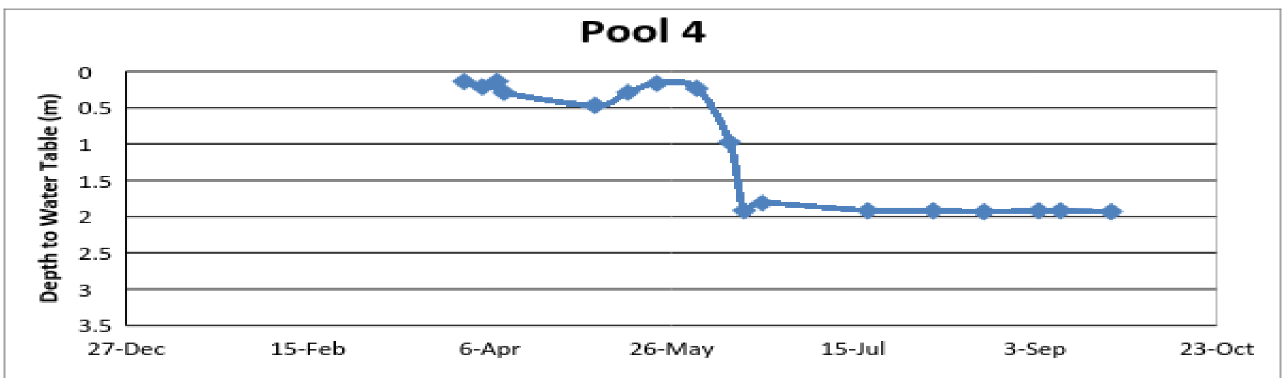
Pool 4
Depth to Water Table (m)
0
0.5
1
1.5
2
2.5
3
3.5
27-Dec
15-Feb
6-Apr
26-May
15-Jul
3-Sep
23-Oct

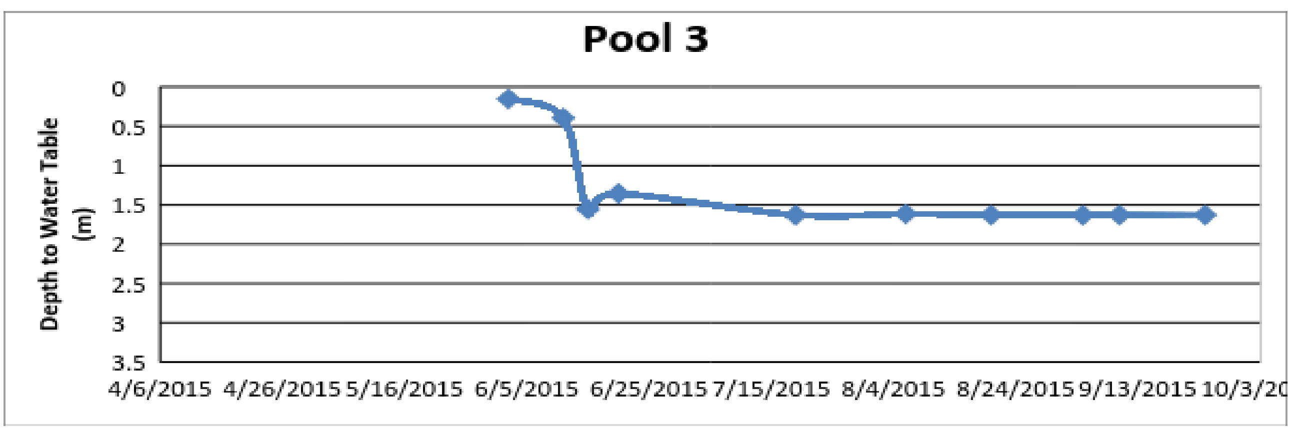
Pool 3
Depth to Water Table (m)
0
0.5
1
1.5
2
2.5
3
3.5
4/6/2015
4/26/2015
5/16/2015
6/5/2015
6/25/2015
7/15/2015
8/4/2015
8/24/2015
9/13/2015

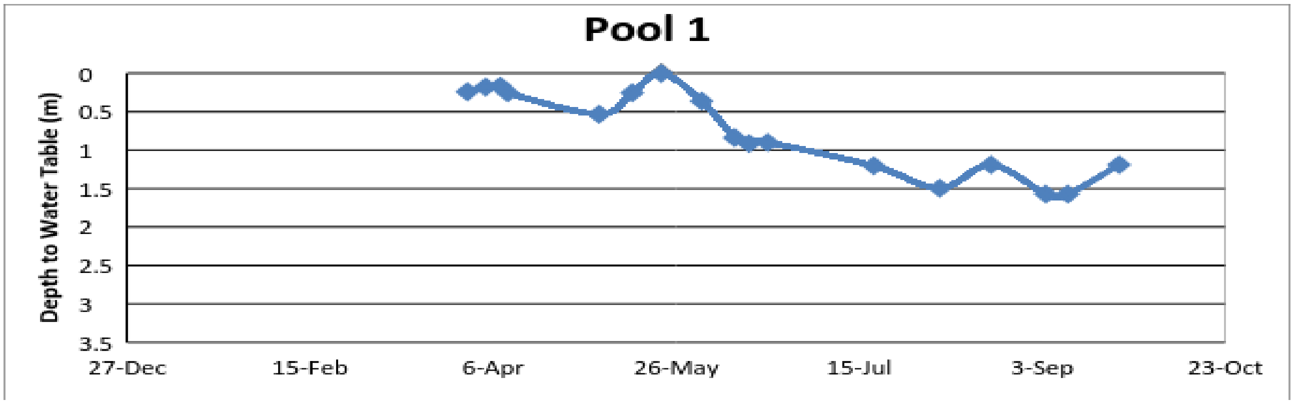

2) Infiltration Measurments

Pool #16	Trial #1	Trial #2	Trial #3
Ring Radius (cm)	15.56	15.56	15.56
Area (cm^2)	7.60E+02	7.60E+02	7.60E+02
Volume (initial)	8.69E+03	3.86E+03	3.86E+03
Volume (final)	7.48E+03	2.65E+03	2.41E+03
Volume Diff	1.21E+03	1.21E+03	1.45E+03
Infiltration Rate (cm/s)	2.22E-06	2.22E-06	2.66E-06
Infiltration Rate (cm/hr)	7.98E-03	7.98E-03	9.58E-03
Standard Deviation	9.22E-04	Variance	8.50E-07

Pool #13	Trial #1	Trial #2	Trial #3
Ring Radius (cm)	15.56	15.56	15.56
Area (cm^2)	7.60E+02	7.60E+02	7.60E+02
Volume (initial)	3.86E+03	4.10E+03	3.86E+03
Volume (final)	1.21E+03	3.14E+03	1.45E+03
Volume Diff	2.66E+03	9.66E+02	2.41E+03
Infiltration Rate (cm/s)	4.88E-06	1.77E-06	4.43E-06
Infiltration Rate (cm/hr)	1.76E-02	6.38E-03	1.60E-02
Standard Deviation	6.04E-03	Variance	3.65E-05

Pool #8	Trial #1	Trial #2	Trial #3
Ring Radius (cm)	15.56	15.56	15.56
Area (cm^2)	7.60E+02	7.60E+02	7.60E+02
Volume (initial)	4.10E+03	3.86E+03	3.86E+03
Volume (final)	2.41E+03	3.14E+03	2.17E+03
Volume Diff	1.69E+03	7.24E+02	1.69E+03
Infiltration Rate (cm/s)	3.10E-06	1.33E-06	3.10E-06
Infiltration Rate (cm/hr)	1.12E-02	4.79E-03	1.12E-02
Standard Deviation	3.69E-03	**Variance**	1.36E-05

Pool #4	Trial #1	Trial #2	Trial #3
Ring Radius (cm)	15.56	15.56	15.56
Area (cm^2)	7.60E+02	7.60E+02	7.60E+02
Volume (initial)	4.10E+03	3.86E+03	4.10E+03
Volume (final)	7.24E+02	9.65E+02	1.21E+03
Volume Diff	3.38E+03	2.90E+03	2.90E+03
Infiltration Rate (cm/s)	6.21E-06	5.32E-06	5.32E-06
Infiltration Rate (cm/hr)	2.24E-02	1.92E-02	1.92E-02
Standard Deviation	1.84E-03	**Variance**	3.40E-06

3) Pressure Transducer Data

a) Sample calculation of water table depth

Plot Title: pool1gw								
#	Date Time, GMT-04:00	Abs Pres, kPa	Temp, °C	Atmospheric Pressure (kPa)	Diff	Density of H20 (Temp Cor)	Water level (m)	Depth from Surface (m)
1	9/24/15 12:28 PM	102.247	21.473	102.233	0.014	997.9185	0.0014	2.2592
2	9/24/15 12:30 PM	102.243	22.717	102.236	0.007	997.6351	0.0007	2.2599
3	9/24/15 12:32 PM	102.299	22.908	102.219	0.08	997.5902	0.0082	2.2524
4	9/24/15 12:34 PM	102.335	23.677	102.236	0.099	997.4058	0.0101	2.2505
5	9/24/15 12:36 PM	102.363	24.158	102.236	0.127	997.2875	0.0130	2.2476
6	9/24/15 12:38 PM	103.23	24.062	102.222	1.008	997.3113	0.1031	2.1575
7	9/24/15 12:40 PM	103.246	22.621	102.239	1.007	997.6575	0.1030	2.1576
8	9/24/15 12:42 PM	103.239	21.664	102.224	1.015	997.8760	0.1038	2.1568
9	9/24/15 12:44 PM	103.274	20.996	102.224	1.05	998.0230	0.1074	2.1532
10	9/24/15 12:46 PM	103.28	20.519	102.227	1.053	998.1252	0.1077	2.1529
11	9/24/15 12:48 PM	103.234	20.043	102.227	1.007	998.2248	0.1029	2.1577
12	9/24/15 12:50 PM	103.159	19.758	102.229	0.93	998.2832	0.0951	2.1655
13	9/24/15 12:52 PM	103.154	19.567	102.212	0.942	998.3220	0.0963	2.1643
14	9/24/15 12:54 PM	103.15	19.377	102.232	0.918	998.3601	0.0938	2.1668
15	9/24/15 12:56 PM	103.145	19.187	102.232	0.913	998.3978	0.0933	2.1673
16	9/24/15 12:58 PM	103.141	18.996	102.249	0.892	998.4354	0.0912	2.1694
17	9/24/15 1:00 PM	103.121	18.901	102.232	0.889	998.4539	0.0909	2.1697
18	9/24/15 1:02 PM	103.119	18.806	102.235	0.884	998.4724	0.0903	2.1703
19	9/24/15 1:04 PM	103.117	18.711	102.218	0.899	998.4907	0.0919	2.1687
20	9/24/15 1:06 PM	103.117	18.711	102.218	0.899	998.4907	0.0919	2.1687

b) Water Table Elevation Time Series

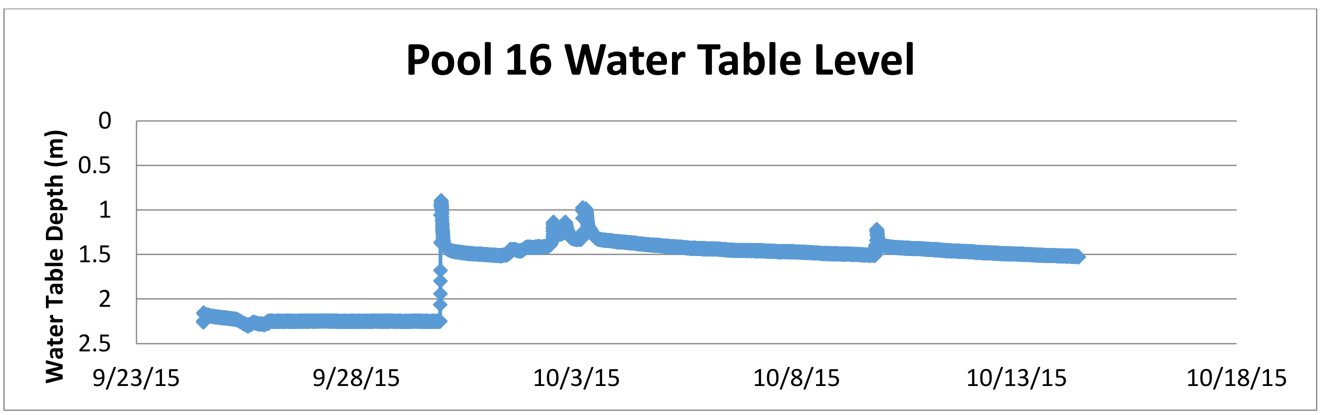

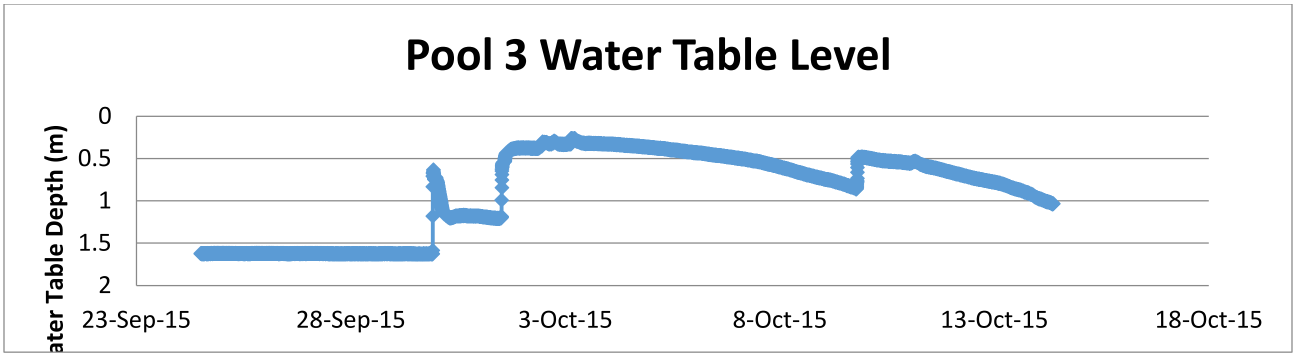
Pool 3 Water Table Level
Water Table Depth (m)
0
0.5
1
1.5
2
23-Sep-15
28-Sep-15
3-Oct-15
8-Oct-15
13-Oct-15
18-Oct-15

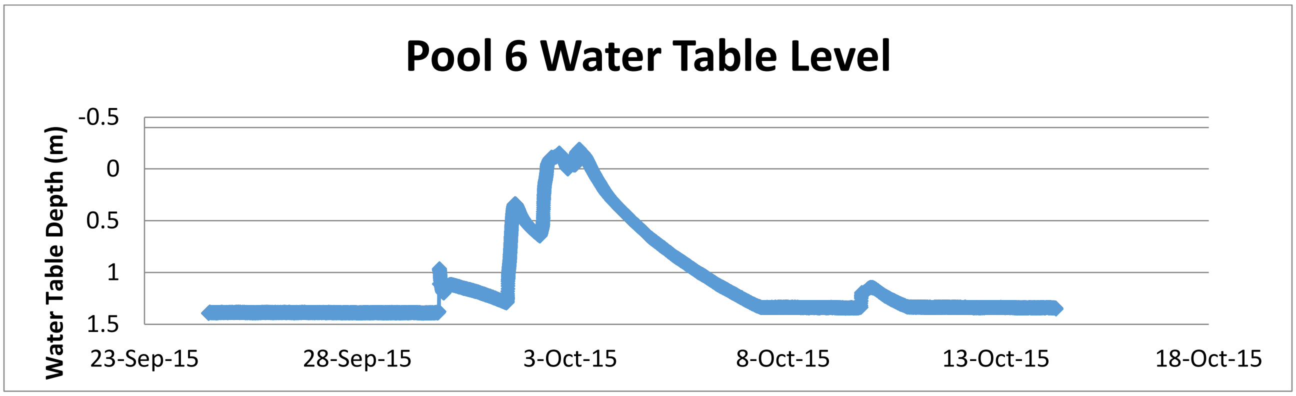
Pool 6 Water Table Level
Water Table Depth (m)
-0.5
0
0.5
1
1.5
23-Sep-15
28-Sep-15
3-Oct-15
8-Oct-15
13-Oct-15
18-Oct-15

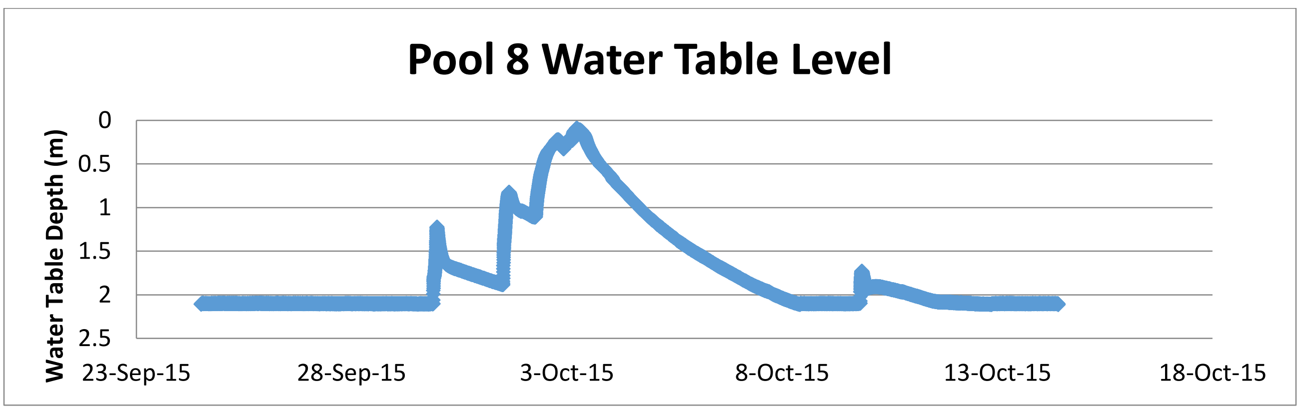
Pool 8 Water Table Level
Water Table Depth (m)
0
0.5
1
1.5
2
2.5
23-Sep-15
28-Sep-15
3-Oct-15
8-Oct-15
13-Oct-15
18-Oct-15

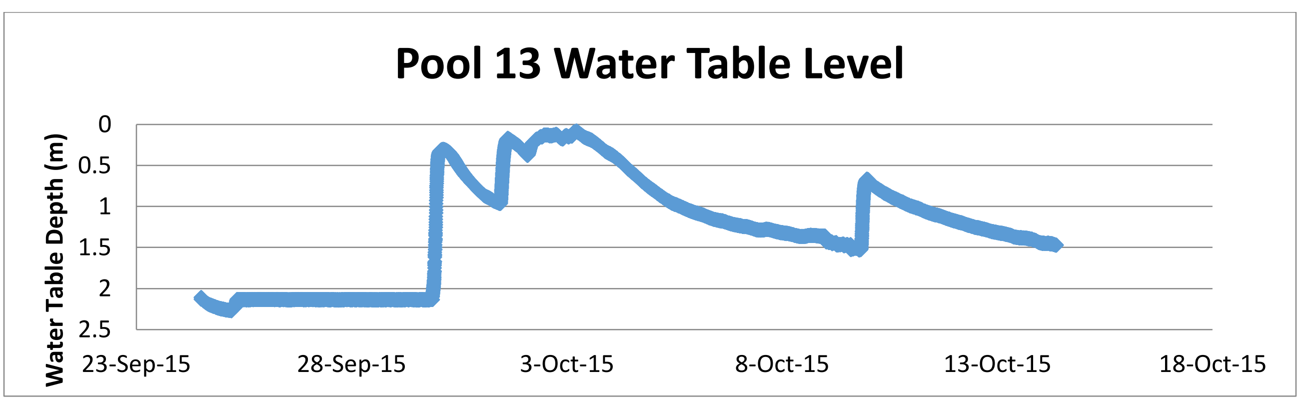
Pool 13 Water Table Level
Water Table Depth (m)
0
0.5
1
1.5
2
2.5
23-Sep-15
28-Sep-15
3-Oct-15
8-Oct-15
13-Oct-15
18-Oct-15

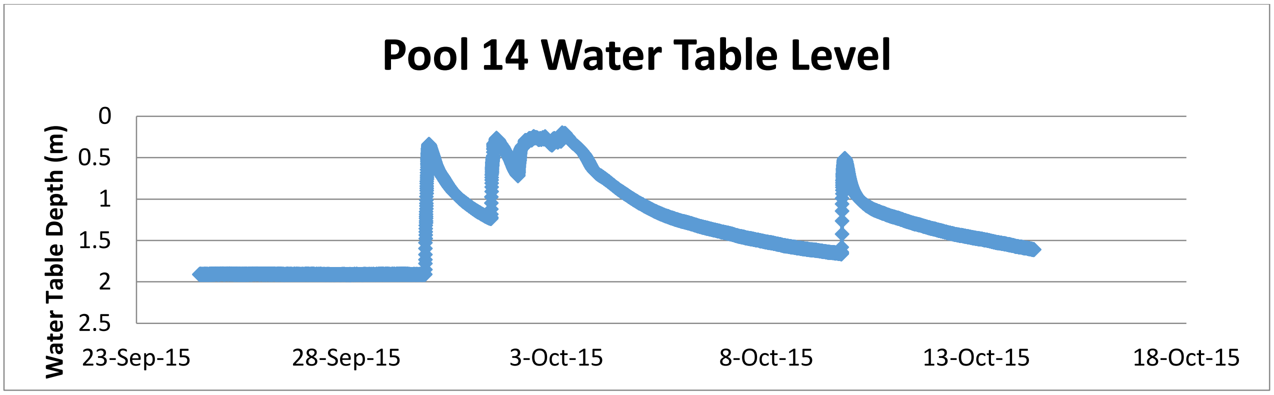
Pool 14 Water Table Level
Water Table Depth (m)
0
0.5
1
1.5
2
2.5
23-Sep-15
28-Sep-15
3-Oct-15
8-Oct-15
13-Oct-15
18-Oct-15

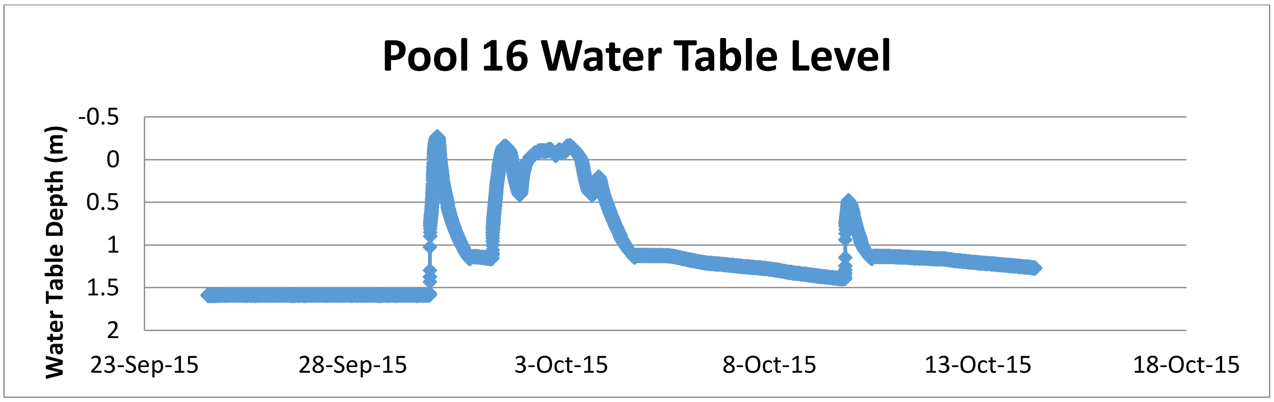
Pool 16 Water Table Level
Water Table Depth (m)
-0.5
0
0.5
1
1.5
2
23-Sep-15
28-Sep-15
3-Oct-15
8-Oct-15
13-Oct-15
18-Oct-15

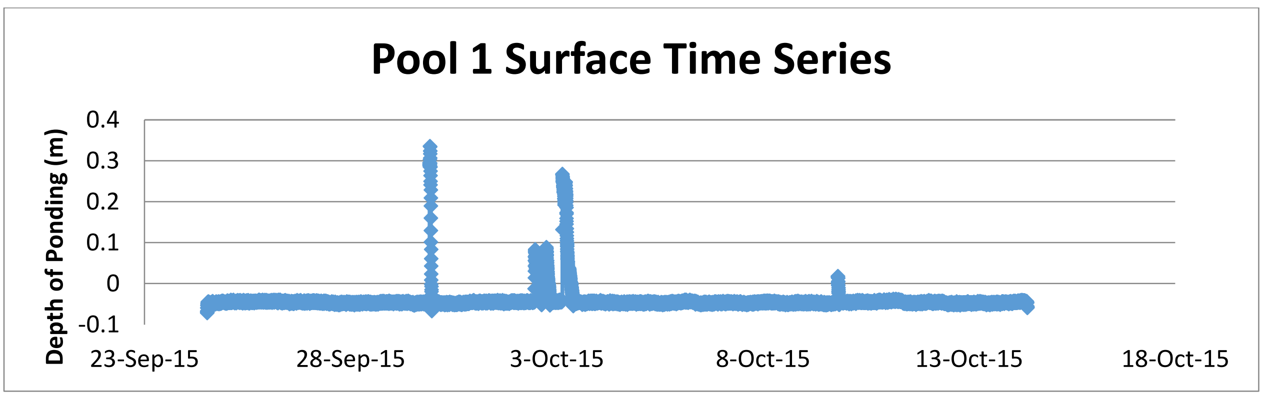
Pool 1 Surface Time Series
Depth of Ponding (m)
0.4
0.3
0.2
0.1
0
-0.1
23-Sep-15
28-Sep-15
3-Oct-15
8-Oct-15
13-Oct-15
18-Oct-15

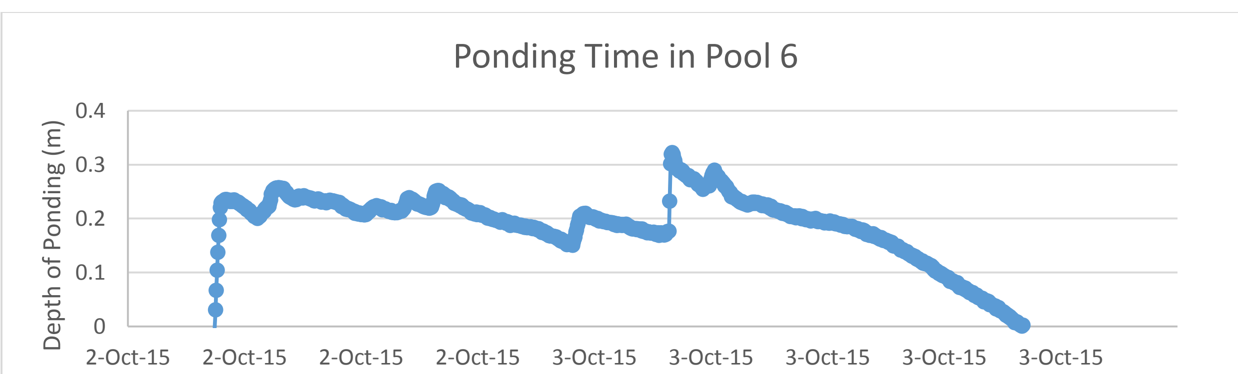
Ponding Time in Pool 6
Depth of Ponding (m)
0.4
0.3
0.2
0.1
0
2-Oct-15
2-Oct-15
2-Oct-15
2-Oct-15
3-Oct-15
3-Oct-15
3-Oct-15
3-Oct-15
3-Oct-15

4) Grain Size Analysis

Pool 8, Depth 8-24"			
size, mm	weight, g	%	cum % finer
32			
22.5			
16			
11.5	0	0	100
8	0.6	0.400534045	99.599466
4	5.9	3.93858478	95.6608812
2	9.9	6.608811749	89.0520694
1	15.6	10.41388518	78.6381842
0.85	10.9	7.276368491	71.3618158
0.5	42	28.03738318	43.3244326
0.25	51	34.04539386	9.27903872
0.125	10.4	6.94259012	2.3364486
0.063	2.4	1.602136182	0.73431242
0.03	1.1	0.734312417	

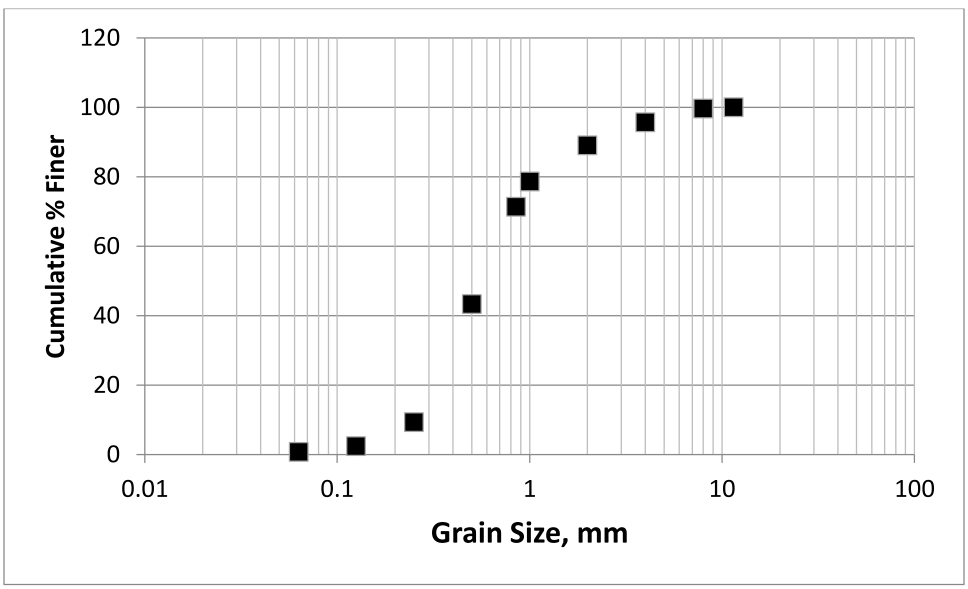

Pool 8 Surface			
size, mm	weight, g	%	cum % finer
32			
22.5			100
16	9.2	5.710738672	94.2892613
11.5	3.9	2.420856611	91.8684047
8	10.2	6.331471136	85.5369336
4	21.5	13.34574798	72.1911856
2	12.7	7.883302297	64.3078833
1	11.8	7.324643079	56.9832402
0.85	3.8	2.358783364	54.6244569
0.5	27	16.75977654	37.8646803
0.25	41	25.45003104	12.4146493
0.125	10.4	6.455617629	5.95903166
0.063	5.9	3.662321539	2.29671012
0.03	3.7	2.296710118	

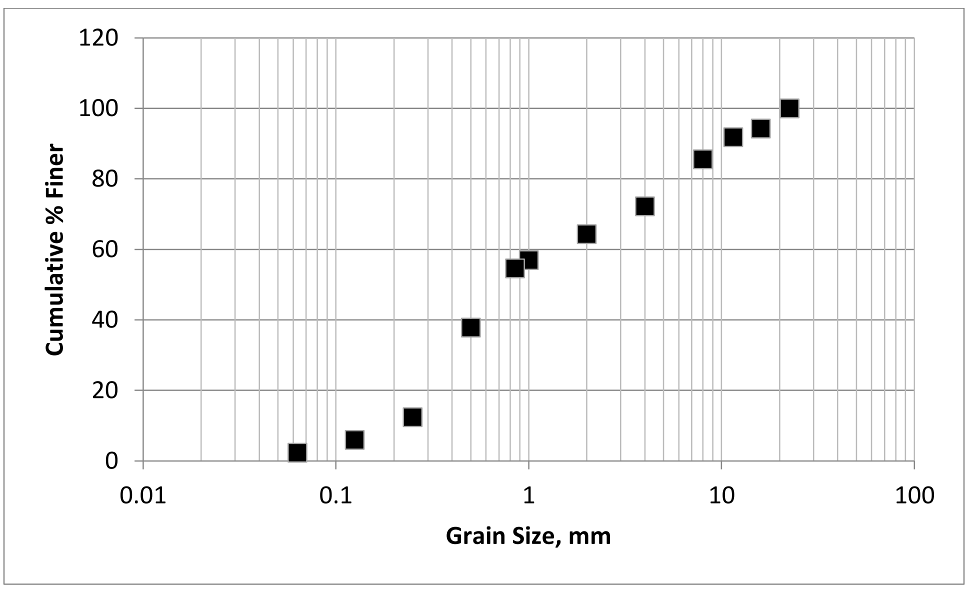

Pool 14 Surface			
size, mm	weight, g	%	cum %
32			
22.5			
16			100
11.5	2	1.10314396	98.89686
8	1.2	0.661886376	98.23497
4	2.8	1.544401544	96.69057
2	6.2	3.419746277	93.27082
1	11.4	6.287920574	86.9829
0.85	4.7	2.592388307	84.39051
0.5	42.4	23.38665196	61.00386
0.25	71.9	39.65802537	21.34584
0.125	22.4	12.35521236	8.990623
0.063	12	6.618863762	2.37176
0.03	4.3	2.371759515